

Decentralized Federated Learning by Partial Message Exchange

Shan Sha, Shenglong Zhou, Xin Wang, Lingchen Kong, Geoffrey Ye Li, *IEEE Fellow*

Abstract—Decentralized federated learning (DFL) has emerged as a transformative server-free paradigm that enables collaborative learning over large-scale heterogeneous networks. However, it continues to face fundamental challenges, including data heterogeneity, restrictive assumptions for theoretical analysis, and degraded convergence when standard communication- or privacy-enhancing techniques are applied. To overcome these drawbacks, this paper develops a novel algorithm, PaME (DFL by Partial Message Exchange). The central principle is to allow only randomly selected sparse coordinates to be exchanged between two neighbor nodes. Consequently, PaME achieves substantial reductions in communication costs while still preserving a high level of privacy, without sacrificing accuracy. Moreover, grounded in rigorous analysis, the algorithm is shown to converge at a linear rate under the gradient to be locally Lipschitz continuous and the communication matrix to be doubly stochastic. These two mild assumptions not only dispense with many restrictive conditions commonly imposed by existing DFL methods but also enables PaME to effectively address data heterogeneity. Furthermore, comprehensive numerical experiments demonstrate its superior performance compared with several representative decentralized learning algorithms.

Index Terms—Partial message exchange, data heterogeneity, communication efficiency-privacy-accuracy, local Lipschitz continuity, linear convergence rate

I. INTRODUCTION

DECENTRALIZED federated learning (DFL) has emerged as a popular paradigm driven by advances in communication technologies and distributed optimization. It is widely regarded as a fundamental framework for peer-to-peer, large-scale collaborative learning and has been systematically reviewed in several recent surveys [1, 2]. Its applications span a wide range of scenarios, including the Internet of Things [3], edge computing [4], and privacy-sensitive industrial domains such as energy [5] and healthcare [6].

A central goal of federated learning is to balance communication efficiency, privacy, and model accuracy. Compared to centralized federated learning (CFL), DFL eliminates the need for a central server, which otherwise constitutes a communication bottleneck and a single point of failure.

This work was supported by the Scientific Research Innovation Capability Support Project for Young Faculty, Fundamental Research Funds for the Central Universities, and the Talent Fund of Beijing Jiaotong University.

Shan Sha, Shenglong Zhou, Xin Wang, and Lingchen Kong are with the School of Mathematics and Statistics, Beijing Jiaotong University, Beijing, China. E-mail: {shansha, shlzhou, xinwang2, lchkong}@bjtu.edu.cn. Geoffrey Ye Li are with the Department of Electrical and Electronic Engineering, Faculty of Engineering, Imperial College London, London, U.K. E-mail: geoffrey.li@imperial.ac.uk.

Corresponding author: Shenglong Zhou.

Moreover, DFL can operate over diverse and possibly time-varying communication topologies, enabling the modeling of heterogeneous and dynamic environments. From a graph-theoretic perspective, CFL can be viewed as a special case of DFL with a star-shaped communication network/graph. These properties generally make DFL more communication-efficient than CFL, especially in large-scale or highly heterogeneous networks. From a privacy perspective, the decentralized setting provides a natural advantage over CFL because it does not require all participants to trust a single central server, which represents a critical vulnerability during training. In contrast, DFL mitigates this risk through its flexible topology: even if an individual node in the network is corrupted, it can be easily isolated (e.g., taken offline), and moderately affects the overall training process. Finally, according to [7, 8], DFL can empirically achieve convergence performance in terms of accuracy comparable to, or in some cases superior to, CFL.

Consequently, DFL offers a more favorable communication efficiency-privacy-accuracy trade-off than CFL. However, this improved architecture comes at the cost of additional complexity in both algorithm design and performance analysis. Requiring no central server implies the absence of a unique global solution at each iteration, and as a result, necessitates the management of local parameters for each node. This, in turn, complicates both the theoretical analysis and robust privacy guarantees. In this work, we propose a DFL algorithm with a novel message exchange mechanism that improves trade-off among communication efficiency, privacy, and accuracy.

A. Related Work

A typical iteration of DFL algorithms alternates between local updates and parameter exchange with neighbor nodes. For instance, as a representative method, D-PSGD [7] combines local stochastic gradient descent (SGD) with neighbor averaging and achieves convergence rates comparable to centralized approaches under some ideal conditions while avoiding server-induced communication bottlenecks. Subsequently, a number of variants have been proposed, mainly by modifying three core components: neighbor selection, parameter aggregation, and local update. We provide a structured review according to these three stages.

1) *Neighbor Selection*: DFL algorithms rely on an underlying communication topology that specifies with which nodes information is exchanged. Common choices of topology include fully connected, ring, and grid networks [9]. Moreover, dynamic communication graphs can be incorporated to enhance flexibility and performance, such as stochastic

communication among nodes via a sampling-based neighbor selection scheme [10], epidemic learning to accelerate model convergence [11], and an adaptive method to identify helpful neighbors [12]. In general, highly connected networks facilitate faster consensus but incur higher communication overhead, whereas sparse or random topologies reduce the communication overhead at the risk of slower convergence. Furthermore, the neighbor-selection strategy can affect the strength of privacy preservation [13].

2) *Parameter Aggregation*: After receiving parameters from neighboring nodes, the next step is to efficiently exploit this information to strengthen consensus and accelerate global convergence. A common strategy is to perform a weighted average over neighboring nodes [14]. Moreover, parameter aggregation is typically the primary step at which communication occurs; thus, various data-compression strategies can be applied to the transmitted signals (e.g., model differences, gradients, or consensus variables) to reduce communication volume. Examples include difference compression [15], gradient sparsification [16], and one-bit compression [17]. To deal with transmission failures, a completion strategy has been proposed in [18] by replacing the lost packets with local parameters at each device.

Additionally, parameter aggregation is a natural stage for incorporating privacy-preserving mechanisms, which can be broadly categorized into encryption-based and differential privacy (DP)-based approaches. The former leverages secure computation and cryptographic techniques, such as secure aggregation and homomorphic encryption [19, 20]. The latter is favored for its formal privacy guarantees and flexibility [21, 22]. However, the DP framework typically requires noise injection, which inevitably introduces an accuracy-privacy trade-off. Therefore, recent work aims to balance this trade-off and mitigate the resulting utility degradation [23].

3) *Local Update*: Following the communication phase, each node performs one or more local updates using its own data. One of the most common frameworks is SGD: each node computes a local stochastic gradient based on its current parameter (usually after aggregation) and updates its model accordingly. Another important class of methods is based on the alternating direction method of multiples (ADMM)-type steps, which have been employed in CFL [24]. However, in decentralized settings, the higher per-iteration complexity has limited their practice. Moreover, several variants of SGD have been developed to accelerate convergence and reduce communication overhead, such as, momentum terms integrated into local updates to improve stability under nonconvex landscapes [25] and multiple local updates between communication rounds to reduce the overall communication cost [26].

B. Contributions

In this work, we address the critical challenge of balancing communication efficiency, accuracy, and privacy preservation in decentralized systems by introducing a partial message exchange (PME, see Fig. 1 or Algorithm 2) mechanism within a DFL algorithm (see Algorithm 1), which hence we term PaME. As presented in Table II, PaME differs from existing

TABLE I: Assumptions for convergence: ①: Convexity; ②: Strong convexity; ③: Lipschitz continuity of the gradient; ④: Bounded (stochastic) gradient or the second-moment of the (stochastic) gradient; ⑤: Bounded variance; ⑥: Lipschitz continuity of the gradient on a bounded region; ⑦: Unbiased gradient estimation; ⑧: Unbiased compression operator; ⑨: Lipschitz continuity of the objective function; ⑩: Bounded compression-error operator; ⑪: Doubly stochastic communication matrix and spectral gap; ⑫: PL condition.

Techniques for communication efficiency: ⑬: Data compression; ⑭: Communication round reduction.

Algorithms	Refs.	Communication	Convergence rate	Assumptions
Type I convergence: $\ \nabla f(\mathbf{w}^T)\ ^2 = B$				
D-PSGD	[7]	none	$O(1/\sqrt{T})$	③⑤⑩
CHOCO-SGD	[27]	⑬	$O(1/T^{\frac{2}{3}})$	③④⑤⑩⑪
SQuARM-SGD	[28]	⑬	$O(1/\sqrt{T})$	③④⑤⑦⑩⑪
DFedSAM	[8]	⑭	$O(1/\sqrt{T})$	③④⑤⑩
EL	[11]	⑭	$O(1/\sqrt{T})$	③④⑤⑦
DCD-PSGD	[15]	⑬	$O(1/\sqrt{T})$	③④⑤⑧⑩
BEER	[29]	⑬	$O(1/T)$	③⑤⑦⑩⑪
Type II convergence: $f(\mathbf{w}^T) - f^\infty = B$				
DFedAvgM	[25]	⑬	$O(1/T)$	③④⑤⑩⑫
DMGT-SVRG	[30]	⑭	$O(\gamma^T)$	②⑦⑨⑩
BEER	[29]	⑬	$O(\gamma^T)$	③⑤⑦⑩⑪⑫
NIDS	[31]	none	$O(\gamma^T)$	②③⑩
ANQ-NIDS	[32]	⑬	$O(\gamma^T)$	②③⑩⑪
PaME	ours	⑬⑭	$O(\gamma^T)$	⑥⑩

DFL algorithms by substantially relaxing theoretical assumptions while achieving a favorable trade-off among communication efficiency, accuracy, and privacy. Our main contributions are summarized as follows.

a) *Convergence under the weakest assumptions*: PaME is proven to converge under two assumptions: Lipschitz continuity of the gradients on a bounded region and the communication matrix to be doubly stochastic. The former is equivalent to the locally Lipschitz continuity, and thus much weaker than the (global) Lipschitz continuity. Moreover, we do not impose additional standard stochastic-gradient assumptions, such as bounded stochastic gradients or variance, which are typically invoked to control stochasticity and client variability. Such a success lies in the establishment of the boundedness of the iterations generated by PaME from a deterministic perspective, despite the algorithm being a stochastic-gradient-based method. Consequently, PaME can effectively handle applications with heterogeneous data.

As summarized in Table II, PaME attains a Type-II convergence guarantee, characterizing the decay of the objective function value. This is often more directly aligned with optimization error compared to Type-I convergence that controls the length of the gradient, i.e., $\|\nabla f(\mathbf{w}^T)\|$, where T is the total iteration number and f^∞ is the optimal value or the limiting point of sequence $\{f(\mathbf{w}^k)\}$. Under two mild assumptions, PaME converges (in Type-II sense) at a linear rate of $O(\gamma^T)$ for some $\gamma \in (0, 1)$, a faster rate than $O(1/T)$ and $O(1/T^2)$. To the best of our knowledge, existing linear convergence results for DFL typically rely on strong convexity [30–32] or

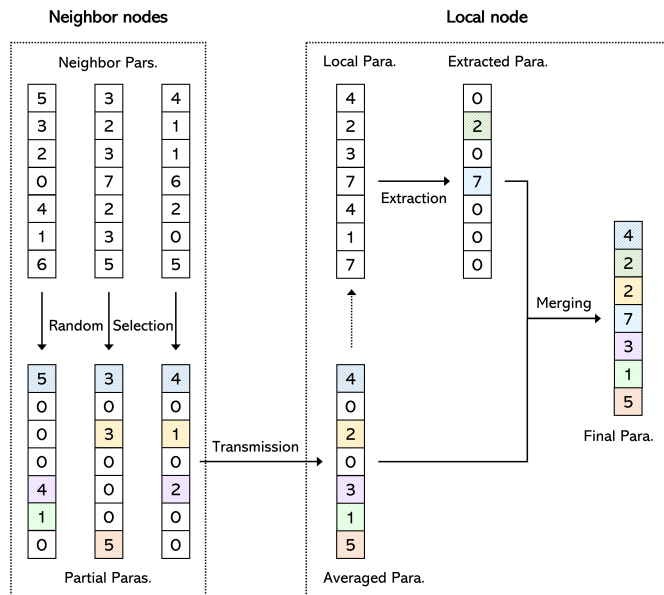


Fig. 1: Partial message exchange (PME) : Every neighbor of a local node i randomly selects partial coordinates (or messages) and transmits them to node i . Node i averages the received incomplete parameters and fills in the missing coordinates using the coordinates in its own local parameter.

PL-type conditions [29], together with additional stochastic-gradient or mixing assumptions, see Table II.

Additionally, since the PME mechanism is intrinsically a form of data compression, our analysis does not rely on the standard unbiased-compressor assumption [15]; its effect can be directly tracked through the iterate dynamics.

Finally, PaME naturally accommodates time-varying communication graphs, which results in dynamic communication matrices at each communication round. Despite this, convergence of PaME is guaranteed provided that only the initial communication matrix is doubly stochastic. This contrasts with many existing DFL methods, which typically require the communication matrices to remain static and doubly stochastic at each communication round [25, 29–32]. This indicates that PaME achieves the convergence in a more complex scenario, where the communication matrices can be dynamic, sparse, and non-doubly stochastic.

b) Communication efficiency: One of the major achievements in this paper lies in the development of the PME mechanism, as outlined in Fig. 1, which enables PaME to reduce the communication cost significantly. Moreover, PaME supports asynchronous updates and multiple local steps between communication rounds, which further increases its flexibility and enables more efficient use of limited communication resources. Overall, the communication efficiency stems from two factors: reduced transmitted content per communication round and reduced communication rounds.

c) Privacy preservation: The PME mechanism and the partial device participation strategy can further contribute to privacy preservation. First, they introduce two layers of randomness (i.e., random neighbor selection and random co-

ordinate sampling) so that each round reveals only partial, obfuscated information. This complicates adversarial tracking or reconstruction of individual samples, consistent with observations in [33]. Furthermore, random coordinate transmission acts as a sparsification scheme that subsamples the parameter dimension: lower information density leads to lower functional sensitivity, which allows for smaller noise magnitudes when combined with privacy-preserving mechanisms such as DP [34] or secure aggregation [35].

d) Robustness: Within the PaME framework, a partial device participation strategy is employed, namely, each local node communicates only with a subset of its selected neighbors. As a result, this design mitigates the impact of stragglers because neighbors with unreliable or slow communication links (i.e., stragglers) can be contacted less frequently or omitted in specific rounds. Moreover, each local node communicates independently according to its own interval, without being affected by other nodes' communication schedules, thereby naturally inducing a partially synchronized training regime and yielding more stable and robust learning dynamics.

e) Superior numerical performance: Extensive numerical experiments are conducted to validate the effectiveness of PaME in comparison with several established DFL algorithms on both synthetic and real-world datasets under data distributions ranging from homogeneous to highly heterogeneous settings. The experimental results demonstrate that PaME achieves a more favorable trade-off between communication efficiency and model accuracy across these scenarios, thereby confirming its robustness to data heterogeneity.

C. Organization

This paper is organized as follows. Section II introduces the mathematical notation and formulates the DFL model. Section III details the proposed algorithm and analyzes its advantages regarding communication efficiency and privacy preservation. Section IV presents the theoretical analysis, including convergence guarantees and complexity analysis. Section V reports experimental results on synthetic and real datasets. Finally, Section VI provides concluding remarks.

II. PRELIMINARIES

We begin this section by presenting the mathematical notation used throughout the paper, followed by the formulation of the optimization model for DFL.

A. Notation

Scalars, vectors, and matrices are written in lowercase, bold lowercase, and bold uppercase letters, respectively, e.g., n , σ , σ_i , and σ_i^k are scalars, \mathbf{w} , \mathbf{w}_i , \mathbf{w}_i^k , \mathbf{g}_i , \mathbf{v} , and $\bar{\mathbf{v}}_i$ are vectors, and \mathbf{W} , \mathbf{W}^α , and \mathbf{V} are matrices. Let $[m] := \{1, 2, \dots, m\}$ and \mathbb{R}^n be the n -dimensional Euclidean space equipped with inner product $\langle \mathbf{w}, \mathbf{v} \rangle := \sum_{t=1}^n w_t v_t$, where ' $:=$ ' means 'is defined as'. Let $\|\cdot\|$ denote the Euclidean norm for vectors and spectral norm for matrices, and $\|\cdot\|_F$ denote the Frobenius norm for matrices. Write w_t , w_{it} , and w_{it}^k to represent the t th entry of vectors \mathbf{w} , \mathbf{w}_i , and \mathbf{w}_i^k , respectively. The cardinality

of a set Ω is denoted by $|\Omega|$. Let $\mathbb{E}(\cdot)$ be the expectation operator. Finally, we use the compact notation

$$\begin{aligned} \mathbf{W} &= (\mathbf{w}_1, \mathbf{w}_2, \dots, \mathbf{w}_m), & \mathbf{V} &= (\bar{\mathbf{v}}_1, \bar{\mathbf{v}}_2, \dots, \bar{\mathbf{v}}_m), \\ \mathbf{G} &= (\mathbf{g}_1, \mathbf{g}_2, \dots, \mathbf{g}_m), & \boldsymbol{\sigma} &= (\sigma_1, \sigma_2, \dots, \sigma_m), \end{aligned}$$

and apply the same convention to define \mathbf{W}^α , \mathbf{V}^α , \mathbf{G}^α , and $\boldsymbol{\sigma}^\alpha$, where α is an integer representing the α th iteration.

B. Decentralized Federated Learning

Given a network of m nodes indexed by $[m]$, each node i has a private dataset \mathcal{D}_i and minimizes a local loss function $f_i(\cdot) := f_i(\cdot; \mathcal{D}_i)$, where $f_i: \mathbb{R}^n \rightarrow \mathbb{R}$ is continuously differentiable and bounded from below. Then the DFL optimization problem can be formulated as

$$\min_{\mathbf{w} \in \mathbb{R}^n} f(\mathbf{w}) := \sum_{i=1}^m f_i(\mathbf{w}), \quad (1)$$

where $\mathbf{w} \in \mathbb{R}^n$ denotes the global parameter to be learned.

Under the decentralized setting, each node maintains a local model parameter \mathbf{w}_i , and model consensus is achieved through peer-to-peer communication. We consider a general communication topology in which node i can exchange messages only with its neighbor nodes $j \in N_i$, where $N_i \subseteq [m]$ denotes the neighbor set of node i . This communication pattern induces an undirected communication graph $G = ([m], E)$, where $E := \{(i, j) : j \in N_i, i \in [m]\}$ is the edge set. To ensure that all nodes eventually reach a common model, namely, $\mathbf{w}_1 = \dots = \mathbf{w}_m = \mathbf{w}$, assume graph G is connected.

Given such a communication topology, model (1) can be equivalently reformulated as the following decentralized optimization problem,

$$\min_{\mathbf{W}} \sum_{i=1}^m f_i(\mathbf{w}_i), \quad \text{s.t. } \mathbf{w}_i = \mathbf{w}_j, (i, j) \in E. \quad (2)$$

The work in this paper is carried out based on the above model.

III. DFL VIA INEXACT ADM

In this section, we first introduce PaME and then highlight several advantageous properties.

A. Algorithm Design

Instead of solving problem (2) directly, we aim to solve the following penalized formulation,

$$\min_{\mathbf{W}} \sum_{i=1}^m \left(f_i(\mathbf{w}_i) + \frac{\sigma_i}{2} \sum_{j \in N_i} \|\mathbf{w}_i - \mathbf{w}_j\|^2 \right),$$

where each $\sigma_i > 0$ is a penalty constant. According to [36], by driving σ_i to ∞ , one can penalize the constraint violations with increasing severity. Therefore, it makes sense to consider m increasing sequence $\{\sigma_i^k\}$, $i \in [m]$ and to seek an approximate minimizer for each k . Specifically, based on current point $\mathbf{W}^k = (\mathbf{w}_1^k, \mathbf{w}_2^k, \dots, \mathbf{w}_m^k)$, one can find an approximate minimizer by solving the following problem,

$$\min_{\mathbf{W}} \sum_{i=1}^m \left(f_i(\mathbf{w}_i) + \frac{\sigma_i^k}{2} \sum_{j \in N_i^k} \|\mathbf{w}_i - \mathbf{w}_j^k\|^2 \right),$$

Algorithm 1 DFL by Partial Message Exchange (PaME)

```

1: Initialize  $\mathbf{w}_i^0 = 0$ , two integers  $\kappa_i > 0$  and  $s_i > 0$ ,  $\sigma_i^0 > 0$ ,
    $\gamma_i > 1$  for each  $i \in [m]$ .
2: for iteration  $k = 0, 1, 2, 3, \dots$  do
3:   for node  $i = 1, 2, \dots, m$  do
4:     if  $k \in \mathcal{K}_i := \{0, \kappa_i, 2\kappa_i, 3\kappa_i, \dots\}$  then
5:       Random neighbor selection:  $N_i^k \subseteq N_i$ .
6:       Neighbor number update:  $m_i^k = |N_i^k|$ .
7:       Partial message exchange:
           
$$\bar{\mathbf{v}}_i^k = \text{PME}(\mathbf{w}_i^k, \{\mathbf{w}_j^k : j \in N_i^k\}).$$

8:     else
9:       Local parameter tracking:  $\bar{\mathbf{v}}_i^k = \mathbf{w}_i^k$ .
10:      Neighbor number tracking:  $m_i^k = m_i^{k-1}$ .
11:    end if
12:    Random sub-batch data sampling:  $\mathcal{B}_i^k \subseteq \mathcal{D}_i$ .
13:    Local parameter updating:
           
$$\mathbf{w}_i^{k+1} = \bar{\mathbf{v}}_i^k - \frac{\nabla f_i(\bar{\mathbf{v}}_i^k; \mathcal{B}_i^k)}{\sigma_i^k m_i^k}. \quad (3)$$

14:    Hyper-parameter increasing:  $\sigma_i^{k+1} = \gamma_i \sigma_i^k$ .
15:  end for
16: end for

```

where $N_i^k \subseteq N_i$ is a randomly selected subset. Solving the above problem is equivalent to address the following m problems independently,

$$\min_{\mathbf{w}_i} f_i(\mathbf{w}_i) + \frac{\sigma_i^k}{2} \sum_{j \in N_i^k} \|\mathbf{w}_i - \mathbf{w}_j^k\|^2, \quad i \in [m]. \quad (4)$$

However, it is still time-consuming to solve the above problem exactly, particularly for complex f_i or high-dimensional settings. An alternative is to solve the above problem inexactly using the linearization of f_i at some point. Based on this, we consider two cases to address problem (4).

- When $k \in \mathcal{K}_i := \{0, \kappa_i, 2\kappa_i, 3\kappa_i, \dots\}$, we require node i to communicate with its selected neighbor nodes $j \in N_i^k$, where κ_i is a positive integer and $N_i^k \subseteq N_i$ is a subset consisting of randomly selected neighbor nodes at the k th iteration. Those neighbor nodes transmit their partial messages \mathbf{v}_j^k defined in (3) to node i based on the rule of PME (i.e., Line 1–4 in Algorithm 2). Then node i averages received message $\{\mathbf{v}_j^k : j \in N_i^k\}$ and its previous parameter \mathbf{w}_i^k to derive an aggregated parameter $\bar{\mathbf{v}}_i^k$ following the rule of (4). Then we linearize f_i at $\bar{\mathbf{v}}_i^k$ and solve problem (4) by

$$\begin{aligned} & \mathbf{w}_i^{k+1} \\ &= \arg \min_{\mathbf{w}_i} \langle \nabla f_i(\bar{\mathbf{v}}_i^k; \mathcal{B}_i^k), \mathbf{w}_i \rangle + \frac{\sigma_i^k}{2} \sum_{j \in N_i^k} \|\mathbf{w}_i - \mathbf{w}_j^k\|^2 \\ &= \bar{\mathbf{v}}_i^k - \frac{1}{\sigma_i^k |N_i^k|} \nabla f_i(\bar{\mathbf{v}}_i^k; \mathcal{B}_i^k), \end{aligned}$$

where \mathcal{B}_i^k is a randomly selected sub-batch data from \mathcal{D}_i .

Algorithm 2 $\bar{\mathbf{v}}_i^k = \text{PME}(\mathbf{w}_i^k, \{\mathbf{w}_j^k : j \in N_i^k\})$

- 1: **for** every node $j \in N_i^k$ **do**
- 2: Random subset selection: $T_j^k \subseteq [n]$ with $|T_j^k| = s_j$.
- 3: Sparse vector \mathbf{v}_j^k generation:

$$v_{j\ell}^k = \begin{cases} w_{j\ell}^k, & \text{if } \ell \in T_j^k, \\ 0, & \text{if } \ell \in T_j^k. \end{cases} \quad (5)$$

- 4: Partial message \mathbf{v}_j^k exchange to node i .
- 5: **end for**
- 6: Node i averages received messages by

$$\bar{v}_{i\ell}^k = \begin{cases} \frac{\sum_{j \in N_i^k} v_{j\ell}^k}{\lambda_{i,\ell}^k}, & \text{if } \lambda_{i,\ell}^k \neq 0, \\ w_{i\ell}^k, & \text{if } \lambda_{i,\ell}^k = 0, \end{cases} \quad (6)$$

for each $\ell \in [n]$, where

$$\lambda_{i,\ell}^k = |\{j \in N_i^k : v_{j\ell}^k \neq 0\}|. \quad (7)$$

- When $k \notin \mathcal{K}_i$ where there is no communication between node i and its neighbor nodes, we linearize f_i at previous point \mathbf{w}_i^k and approximately solve problem (4) by

$$\begin{aligned} & \mathbf{w}_i^{k+1} \\ &= \arg \min_{\mathbf{w}_i} \langle \nabla f_i(\mathbf{w}_i^k; \mathcal{B}_i^k), \mathbf{w}_i \rangle + \frac{\sigma_i^k}{2} \sum_{j \in N_i^k} \|\mathbf{w}_i - \mathbf{w}_j^k\|^2 \\ &= \mathbf{w}_i^k - \frac{1}{\sigma_i^k |N_i^k|} \nabla f_i(\mathbf{w}_i^k; \mathcal{B}_i^k). \end{aligned}$$

In this case, we keep $N_i^k = N_i^{k-1}$.

Overall, by incorporating the above two cases into the DFL framework, we develop the proposed algorithm, termed PaME (**P**artial **M**essage **E**xchange for DFL), as outlined in Algorithm 1. We highlight its main advantages as follows.

B. Partial Message Exchange (PME)

In Algorithm 1, when $k \in \mathcal{K}_i$, node i communicates with its selected neighbors via PME outlined in Algorithm 2. An illustrative example is provided in Fig. 1. The key features of PME are twofold.

- 1) Node $j \in N_i^k$ transmits a sparse vector \mathbf{v}_j^k , namely, s_j randomly selected coordinates in $\mathbf{w}_j^k \in \mathbb{R}^n$ and $(n - s_j)$ zeros, to node i . This can lead significant transmission volume reduction. Specifically, transmitting this sparse vector \mathbf{v}_j^k using double-precision floating-point format requires

$$(64s_j + n - s_j) = (63s_j + n) \text{ bits}. \quad (8)$$

In contrast, transmitting a dense vector $\mathbf{w}_j^k \in \mathbb{R}^n$ with the same format generally requires $(64n)$ bits. When $s_j \ll n$,

$$(63s_j + n) \ll 64n.$$

For example, $1.63 \times 10^4 \ll 6.4 \times 10^5$ if $n = 100s_j = 10^4$. We shall point out that if $w_{j\ell}^k = 0$ for some $\ell \in T_j^k$ in (3) (which is unlikely to happen in practice), then to distinguish this useful 0 and 0 for $\ell \notin T_j^k$, the neighbor could use a

character, such as ‘ \star ’, to replace this useful 0. For example, at k th iteration,

$$\mathbf{w}_5^k = [3, 6, 0, 6]^\top, \quad T_5^k = \{3, 4\}, \quad \mathbf{v}_5^k = [0, 0, \star, 6]^\top.$$

In \mathbf{v}_5^k , there are two useful coordinates, namely, $v_{53}^k = 0$ and $v_{54}^k = 6$. Using such a strategy, the transmission volume would not be affected as we only need 8bits (< 64 bits) to transmit this character ‘ \star ’.

- 2) The averaging mechanism in (4) is novel and yields an unbiased estimator. It averages the ℓ th entry using $\lambda_{i,\ell}^k$ rather than $|N_i^k|$, where $\lambda_{i,\ell}^k$ is defined in (5) and counts the number of $\{\mathbf{v}_j^k : j \in N_i^k\}$ with non-zero entry $v_{j\ell}^k$ (‘ \star ’ is treated as a nonzero). In this way, given $\lambda_{i,\ell}^k > 0$, the ℓ th entry of $\bar{\mathbf{v}}_i^k$ yields an unbiased estimation of the average of selected neighbors’ parameters $\{\mathbf{w}_j^k : j \in N_i^k\}$ under some certain sampling rules, namely,

$$\mathbb{E}(\bar{v}_{i\ell}^k \mid \lambda_{i,\ell}^k > 0) = \frac{1}{|N_i^k|} \sum_{j \in N_i^k} w_{j\ell}^k.$$

In contrast, directly averaging $\{\mathbf{v}_j^k : j \in N_i^k\}$ using $|N_i^k|$, namely $\sum_{j \in N_i^k} \mathbf{v}_j^k / |N_i^k|$, will yields a biased estimation, as shown in the following theory whose proof can be found in Section I of the Supplemental Material.

Theorem 1. *Let $\bar{\mathbf{w}}$ be the average of q vectors $\mathbf{w}_1, \mathbf{w}_2, \dots, \mathbf{w}_q \in \mathbb{R}^n$. For each $i \in [q]$, independently construct a sparse vector $\mathbf{v}_i \in \mathbb{R}^n$ by uniformly selecting s coordinates of \mathbf{w}_i without replacement from $[n]$. Define indicator variables by*

$$\delta_{i\ell} = \begin{cases} 1, & \text{if } w_{i\ell} \text{ is selected,} \\ 0, & \text{otherwise,} \end{cases} \quad \delta_\ell := \sum_{i=1}^q \delta_{i\ell}.$$

and two averages $\bar{\mathbf{v}}$ and $\tilde{\mathbf{v}}$ by

$$\bar{v}_\ell = \begin{cases} \frac{1}{\delta_\ell} \sum_{i=1}^q v_{i\ell}, & \text{if } \delta_\ell > 0, \\ 0, & \text{otherwise,} \end{cases} \quad \tilde{v}_\ell = \frac{1}{q} \sum_{i=1}^q v_{i\ell}$$

for any $\ell \in [n]$. Then

$$\mathbb{E}(\bar{v}_\ell \mid \delta_\ell > 0) = \bar{w}_\ell, \quad \mathbb{E}(\tilde{v}_\ell \mid \delta_\ell > 0) = \frac{s}{n} \bar{w}_\ell. \quad (9)$$

We provide an example to illustrate the above theorem and to detail the computation of $\bar{\mathbf{v}}_i^k = \text{PME}(N_i^k)$ in accordance with Algorithm 2. Suppose that at k th iteration,

$$N_i^k = \{2, 4, 5\}, \quad s_2 = s_4 = s_5 = 2$$

and \mathbf{w}_i^k and $(\mathbf{w}_j^k, T_j^k, \mathbf{v}_j^k), j \in N_i^k$ are given by

$$\begin{aligned} \mathbf{w}_i^k &= [2, 8, 3, 6]^\top, \\ \mathbf{w}_2^k &= [2, 8, 1, 4]^\top, \quad T_2^k = \{1, 4\}, \quad \mathbf{v}_2^k = [2, 0, 0, 4]^\top, \\ \mathbf{w}_4^k &= [4, 7, 2, 5]^\top, \quad T_4^k = \{3, 4\}, \quad \mathbf{v}_4^k = [0, 0, 2, 5]^\top, \\ \mathbf{w}_5^k &= [3, 6, 0, 6]^\top, \quad T_5^k = \{3, 4\}, \quad \mathbf{v}_5^k = [0, 0, \star, 6]^\top, \end{aligned}$$

where T_j^k is randomly selected to such that $|T_j^k| = 2$ and \mathbf{v}_j^k are obtained by (3). According to (5),

$$\lambda_{i,1}^k = 1, \quad \lambda_{i,2}^k = 0, \quad \lambda_{i,3}^k = 2, \quad \lambda_{i,4}^k = 3,$$

namely, in $\mathbf{v}_2^k, \mathbf{v}_4^k, \mathbf{v}_5^k$, the 1, 2, 3, and 4th coordinates contain 1, 0, 2, and 3 effective entries, respectively, as indicated by the underlined elements. Then from (4), we have

$$\bar{\mathbf{v}}_i^k = \left[\frac{2}{1}, (\mathbf{w}_i^k)_2, \frac{2+\star}{2}, \frac{4+5+6}{3} \right]^\top = [2, 8, 1, 5]^\top,$$

where ‘ \star ’ is treated back to 0. The mean of the selected neighbors’ parameters and sparse parameters are computed by

$$\begin{aligned} \tilde{\mathbf{v}}_i^k &= \frac{1}{|N_i^k|} \sum_{j \in N_i^k} \mathbf{v}_j^k = \left[\frac{2}{3}, 0, \frac{2}{3}, 5 \right]^\top, \\ \bar{\mathbf{w}}_i^k &= \frac{1}{|N_i^k|} \sum_{j \in N_i^k} \mathbf{w}_j^k = [3, 7, 1, 5]^\top. \end{aligned}$$

Obviously, $\bar{\mathbf{v}}_i^k$ is a closer estimator to $\bar{\mathbf{w}}_i^k$ than $\tilde{\mathbf{v}}_i^k$.

C. Communication Efficiency

The communication efficiency of PaME in Algorithm 1 arises from three factors.

- Communication between node i and its selected neighbors $N_i^k \subseteq N_i$ occurs only at iterations $k \in \mathcal{K}_i$, rather than at every step. Consequently, a larger period κ_i permits multiple local updates between communication events, thereby reducing the communication rounds. This periodic communication strategy is well-established in [37–43].
- Even at $k \in \mathcal{K}_i$, node i only communicates with a selected subset of its neighbors, rather than all neighbors.
- As discussed earlier, each node $j \in [m]$ only transmits partial messages with $(63s_j + n)$ bits content, instead of the full model parameter with $(64n)$ bits content. This substantially reduces the transmitted message size and, in turn, significantly improves communication efficiency.

D. Privacy Enhancement

The proposed approach guarantees privacy through three principal components:

- The inherent heterogeneity of communication intervals combined with the dynamic nature of the network topology significantly complicates topology inference attacks. Specifically, the temporal variability makes it more challenging for an adversary to reliably reconstruct per-round connectivity or identify persistent communication pathways from observed exchanges.
- The partial message exchange mechanism employs random coordinate subsampling, which reduces the amount of information revealed in each communication round. By exchanging only a sparse, randomized subset of parameters in each round, the algorithm limits the instantaneous information leakage, thereby making it difficult for malicious actors to perform data reconstruction (e.g., gradient inversion) or infer private attributes.
- The framework of PME naturally allows for extension to some privacy-enhancing mechanisms. For instance, it can be combined with the sparse vector technique [44, 45] by setting a thresholding mechanism to determine whether to transmit specific coordinates. Consequently, this integration achieves a superior privacy-utility trade-off by minimizing privacy budget consumption.

E. Robustness

PaME is relatively robust due to two strategies: partial device participation and partial synchronization.

- When communication occurs, each node i selects a subset of neighbor nodes $N_i^k \subseteq N_i$ to participate in training, which helps mitigate the impact of stragglers. Following the approach in [41], node i sets a threshold $m_i^k \in [1, |N_i|)$ and forms N_i^k from the first m_i^k neighbors that respond. Once m_i^k sparse parameters are received, node i proceeds without waiting for the remaining neighbors, which are treated as stragglers in that iteration. In practical deployments, a neighbor j with unreliable or severely delayed communication can therefore be treated as a persistent straggler and excluded from N_i^k , i.e., $j \notin N_i^k$. This mechanism is closely related to partial device participation strategies in CFL [24, 46, 47]. Moreover, Algorithm 1 imposes no specific structural constraint on the communication topology during training. The neighbor sets, N_i^k , may vary over time, and at each communication round node i only needs to synchronize with the currently selected subset N_i^k .
- Each node i communicates independently according to its own interval κ_i , without being affected by other nodes’ communication schedules, thereby naturally inducing a partially synchronized training regime and yielding more stable and robust learning dynamics.

IV. THEORETICAL ANALYSIS

This section provides the theoretical results of the proposed algorithm, including the convergence and complexity.

A. Assumptions and Setup

To establish the convergence of PaME, we introduce two assumptions, before which, let the communication matrix, $\mathbf{B} \in \mathbb{R}^{m \times m}$, be defined by

$$B_{ji} := \begin{cases} \frac{1}{m_i}, & \text{if } j \in N_i, \\ 0, & \text{otherwise,} \end{cases}$$

Assumption 1. \mathbf{B} is doubly stochastic and satisfies

$$\zeta := \max\{|\lambda_2(\mathbf{B})|, |\lambda_m(\mathbf{B})|\} < 1. \quad (10)$$

where $\lambda_i(\mathbf{B})$ is the i th largest eigenvalue of \mathbf{B} .

Regarding Assumption 1, it has been extensively adopted to ensure the convergence of DFL algorithms, see those in Table I. However, it is worth pointing out that PaME in Algorithm 1 naturally accommodates time-varying communication graphs since N_i^k is varying at each communication round (namely, at $k \in \mathcal{K}$), which result in dynamic communication matrices \mathbf{B}^k (defined by $B_{ji}^k = 1/|N_i^k|$ if $j \in N_i^k$ and $B_{ji}^k = 0$ otherwise) at each $k \in \mathcal{K}$. Despite this, convergence of PaME is guaranteed provided that only the initial communication matrix (i.e., \mathbf{B}) is doubly stochastic. This contrasts with many existing DFL methods, which typically require the communication matrices to remain static (namely, $\mathbf{B}^k \equiv \mathbf{B}$) and doubly stochastic at each communication round [25, 29–32]. This indicates that PaME achieves the convergence in a more complex scenario,

where communication matrices \mathbf{B}^k can be dynamic, sparse, and non-doubly stochastic.

Assumption 2. For each $i \in [m]$, ∇f_i is Lipschitz continuous with $\alpha_i > 0$ on $\mathbb{N}(2\delta)$ for a given $\delta \in (0, \infty)$, where

$$\mathbb{N}(2\delta) := \{\mathbf{w} \in \mathbb{R}^n : \|\mathbf{w}\|_\infty \leq 2\delta\}$$

and $\|\mathbf{w}\|_\infty$ denotes the infinity norm of \mathbf{w} .

Regarding Assumption 2, the Lipschitz continuity of the gradient (often referred to as L -smoothness) on a bounded region is equivalent to local Lipschitz continuity. Thus, it is a local version of L -smoothness. This constitutes a substantially weaker condition compared to the global L -smoothness, convexity, or bounded gradient assumptions commonly imposed in standard DFL frameworks (see Table II). As a result, our theoretical findings are established under the mildest conditions among existing DFL convergence guarantees.

For the purpose of simplifying the convergence analysis, we adopt the following parameter settings.

Setup 1. Parameters in Algorithm 1 are chosen as follows.

- 1) Set $\mathbf{W}^0 = \mathbf{0}$ and $\kappa_i = k_0$ for all $i \in [m]$. This is adopted for analytical convenience without loss of generality. In fact, one can always let k_0 be the least common multiple of $\{\kappa_1, \kappa_2, \dots, \kappa_m\}$, then the subsequent analysis remains similar to the case of $\kappa_i = k_0$.
- 2) Set $m_i^k = t_i = \lfloor \nu_i |N_i| \rfloor$ for all $k \geq 0$ and $i \in [m]$, where $\nu_i \in (0, 1]$ is the participation rate and $\lfloor \cdot \rfloor$ is the floor of \cdot . That is, at every iteration, node i selects the same number of neighbor nodes to join in the training.
- 3) Set $\sigma_i^0 = \sigma^0$ and $\gamma_i = \gamma$, $s_i = s$ for all $i \in [m]$. Again, this is adopted for analytical convenience without loss of generality. In fact, for different σ_i^0 and γ_i , we can conduct similar analysis by considering

$$\sigma^0 = \min_i \sigma_i^0, \quad \gamma = \min_i \gamma_i, \quad s = \min_i s_i.$$

Moreover, in Algorithm 2, each node $j \in N_i^k$ independently constructs a set T_j^k by uniformly selecting s entries of $[n]$ without replacement.

- 4) In the sequel, given ζ defined in (6) and integers k_0 and (t_1, \dots, t_m) , initialize the following parameters

$$\gamma \in \left(1, \zeta^{-2/k_0}\right), \quad p := \frac{s}{n} \in (0, 1), \quad \nu_i \in (0, 1], \quad (11)$$

such that

$$(1-p)^{t_i} (1+\zeta)^2 + 2p \sum_{j \in N_i} \nu_j < \left(\gamma^{-k_0/2} - \zeta\right)^2, \quad (12)$$

for any $i \in [m]$. Moreover, choose

$$\sigma^0 \geq \sigma,$$

where $\sigma \in (0, \infty)$ is a given constant relying on α_i , t_i , δ , and γ . Its explicit form are given in Supplemental material.

We would like to point out that since s (i.e., p) and ν_i can be chosen flexibly, there are always many choices of these parameters, for instance, taking p close to 1 and ν_i close to 0, that satisfy condition (11).

B. Sequence Convergence

For notational simplicity, we define two gaps by

$$\Delta \mathbf{w}_i^k := \mathbf{w}_i^k - \mathbf{w}_i^{k-1}, \quad \Delta \bar{\mathbf{v}}_i^k := \bar{\mathbf{v}}_i^k - \bar{\mathbf{v}}_i^{k-1},$$

and a merit function by

$$\begin{aligned} H^k &:= \mathbb{E} \sum_{i=1}^m \left(f_i(\mathbf{w}_i^k) + \frac{\sigma_i^k t_i}{2} \|\mathbf{w}_i^k - \bar{\mathbf{v}}_i^k\|^2 \right), \\ \tilde{H}^k &:= H^k + C\gamma^{-k} + D\eta^{-k}, \\ \varpi^k &:= \frac{1}{m} \sum_{i=1}^m \mathbf{w}_i^k, \end{aligned}$$

where γ is given in (10), $\eta > 1$, $C > 0$, and $D > 0$. The explicit forms of (η, C, D) are given in Supplemental material and do not rely on the generated sequence. The first following result establishes the boundedness of the sequence generated by PaME, as well as the monotonic decreasing property of a sequence associated with H^k .

Theorem 2. Let $\{(\mathbf{W}^k, \mathbf{V}^k)\}$ be the sequence generated by Algorithm 1 with Setup 1. Then the following statements hold under Assumptions 1 and 2.

- 1) For any $k \geq 0$ and $i \in [m]$, $\mathbf{w}_i^k \in \mathbb{N}(2\delta)$ and $\bar{\mathbf{v}}_i^k \in \mathbb{N}(2\delta)$.
- 2) For any $k \geq 0$,

$$\tilde{H}^k - \tilde{H}^{k+1} \geq \mathbb{E} \sum_{i=1}^m \frac{\sigma_i^k t_i}{8} \left(\|\Delta \mathbf{w}_i^{k+1}\|^2 + \|\Delta \bar{\mathbf{v}}_i^{k+1}\|^2 \right),$$

The proof of Theorem 2 is provided in Section III-D of the Supplemental Material. It is worth noting that the boundedness of the generated sequence is a crucial property, as it allows us to relax several commonly imposed boundedness assumptions, such as bounded (stochastic) gradients, bounded second moments of the (stochastic) gradients, and bounded variance, as summarized in Table I. This observation partially explains why the subsequent convergence results can be established under mild assumptions. We provide the main convergence result.

Theorem 3. Let $\{(\mathbf{W}^k, \mathbf{V}^k)\}$ be the sequence generated by Algorithm 1 with Setup 1. Then the following statements hold under Assumptions 1 and 2.

- 1) For any $i \in [m]$,

$$\lim_{k \rightarrow \infty} \mathbb{E} \|\Delta \mathbf{w}_i^k\| = \lim_{k \rightarrow \infty} \mathbb{E} \|\Delta \bar{\mathbf{v}}_i^k\| = \lim_{k \rightarrow \infty} \mathbb{E} \|\mathbf{w}_i^k - \bar{\mathbf{v}}_i^k\| = 0.$$

- 2) Sequence $\{\varpi^k\}$ converges to ϖ^∞ in the sense of L^2 convergence and expectation, namely,

$$\lim_{k \rightarrow \infty} \mathbb{E} \|\varpi^k - \varpi^\infty\|^2 = 0, \quad \lim_{k \rightarrow \infty} \mathbb{E} \varpi^k = \mathbb{E} \varpi^\infty.$$

Sequence $\{(\mathbb{E} \mathbf{W}^k, \mathbb{E} \mathbf{V}^k)\}$ converges and satisfies

$$\lim_{k \rightarrow \infty} \mathbb{E} \mathbf{W}^k = \lim_{k \rightarrow \infty} \mathbb{E} \mathbf{V}^k = (\mathbb{E} \varpi^\infty, \dots, \mathbb{E} \varpi^\infty) =: \mathbf{W}^\infty.$$

- 3) Sequence $\{(H^k, \tilde{H}^k, \mathbb{E} f(\varpi^k))\}$ converges and satisfies

$$\lim_{k \rightarrow \infty} \tilde{H}^k = \lim_{k \rightarrow \infty} H^k = \lim_{k \rightarrow \infty} \mathbb{E} f(\varpi^k) = \mathbb{E} f(\varpi^\infty).$$

The proof of Theorem 3 is provided in Section III-E of the Supplemental Material. We now establish the convergence rate under the same assumptions and parameter setup.

Theorem 4. Let $\{(\mathbf{W}^k, \mathbf{V}^k)\}$ be the sequence generated by Algorithm 1 with Setup 1. Under Assumptions 1 and 2.

$$\begin{aligned} \mathbb{E}\|\mathbf{W}^k - \mathbf{W}^\infty\|_F^2 &= O(\gamma^{-k}), \\ \mathbb{E}\|\mathbf{V}^k - \mathbf{V}^\infty\|_F^2 &= O(\gamma^{-k}), \\ \mathbb{E}|f(\boldsymbol{\varpi}^k) - f(\boldsymbol{\varpi}^\infty)| &= O(\gamma^{-k/2}). \end{aligned}$$

The proof of Theorem 4 is provided in Section III-D of the Supplemental Material. Theorem 4 establishes that both sequences $\{(\mathbf{W}^k, \mathbf{V}^k)\}$ and $\{f(\boldsymbol{\varpi}^k)\}$ converge to their respective limits at a linear rate in the sense of L^2 convergence. We emphasize that the theoretical guarantees, including Theorems 3 and 4, are derived under the randomness induced by the PME mechanism in Algorithm 1. If a deterministic transmission scheme is employed instead, all convergence results hold with probability one, thereby recovering a strong deterministic convergence theory for the standard DFL setting.

V. NUMERICAL EXPERIMENTS

In this section, we present numerical experiments to evaluate the performance of PaME. All experiments are implemented using Python 3.7.

A. Testing Example

Example 1. (Linear Regression): The loss function of each node $i \in [m]$ with a local dataset \mathcal{D}_i takes the following form,

$$f_i(\mathbf{w}) = \frac{1}{2m_i} \sum_{(\mathbf{a}, b) \in \mathcal{D}_i} (\langle \mathbf{a}, \mathbf{w} \rangle - b)^2,$$

where feature $\mathbf{a} \in \mathbb{R}^n$, observation $b \in \mathbb{R}$, $m_i = |\mathcal{D}_i|$. To assess the effectiveness of PaME, we assume the existence of a ‘ground truth’ solution $\mathbf{w}^* \in \mathbb{R}^n$ with 1% non-zeros entries. Then $b = \langle \mathbf{a}, \mathbf{w}^* \rangle + 0.5e$, where e is the noise. All entries of \mathbf{a} and e are identically and independently distributed from a standard normal distribution while the non-zero entries of \mathbf{w}^* are uniformly generated from $[0.5, 2] \cup [-2, -0.5]$.

Example 2. (Logistic Regression): The loss function of each node $i \in [m]$ with a local dataset \mathcal{D}_i takes the following form,

$$f_i(\mathbf{w}) = \frac{1}{m_i} \sum_{(\mathbf{a}, b) \in \mathcal{D}_i} \left(\ln \left(1 + e^{\langle \mathbf{a}, \mathbf{w} \rangle} \right) - b \langle \mathbf{a}, \mathbf{w} \rangle \right) + \frac{\lambda}{2} \|\mathbf{w}\|^2,$$

where feature $\mathbf{a} \in \mathbb{R}^n$, label $b \in \{0, 1\}$, $m_i = |\mathcal{D}_i|$, and $\lambda > 0$ (e.g., $\lambda = 0.001$ in our numerical experiments). We assume a ground-truth parameter vector $\mathbf{w}^* \in \mathbb{R}^n$ with 50% nonzero entries. Let \mathbf{a} be generated in the same way as in Example 1, and b is obtained by applying the sigmoid function to $\langle \mathbf{a}, \mathbf{w}^* \rangle$ to produce a probability in $[0, 1]$.

Example 3. (Convolutional Neural Network, CNN): Consider a 10-class image classification problem trained using a CNN. Each node $i \in [m]$ possesses a local dataset \mathcal{D}_i and minimizes the empirical cross-entropy loss:

$$f_i(\mathbf{w}) = -\frac{1}{m_i} \sum_{(\mathbf{a}, b) \in \mathcal{D}_i} \sum_{c \in [10]} \mathbb{I}(b = c) \ln(h(\mathbf{w}; \mathbf{a})_c),$$

where (\mathbf{a}, b) denotes a training sample (e.g., an image and its corresponding label), $m_i = |\mathcal{D}_i|$, $\mathbb{I}(\cdot)$ is the indicator function,

and $h(\mathbf{w}; \mathbf{a})_c$ is the predicted probability of class c given input \mathbf{a} parametrized by \mathbf{w} .

We utilize the Fashion-MNIST dataset [48], which consists of 70,000 grayscale images (28×28 pixels) depicting 10 categories of fashion items, split into 60,000 training images and 10,000 testing images. To verify the generalizability of PaME under data heterogeneity, we employ data partitioning strategies wherein each node is allocated samples from a varying number of classes, thereby simulating diverse heterogeneous data distributions.

Example 4. (ResNet-20): Consider extending the multi-class classification problem and objective function in Example 3 by replacing the CNN backbone with ResNet-20 [49] and evaluate on CIFAR-10 [50], a more challenging natural-image benchmark. CIFAR-10 consists of 60,000 32×32 color images in 10 classes (e.g., airplane, automobile, bird), with 50,000 training images and 10,000 test images. Compared with Example 3 (Fashion-MNIST), CIFAR-10 typically poses a harder learning task due to the complexity of color natural images and higher intra-class variability. To simulate heterogeneous (non-IID) data across nodes, we adopt a Dirichlet partitioning strategy [8], where the class distribution for each client is sampled from a Dirichlet distribution $\text{Dir}(\beta)$.

B. Implementation

The basic setup for PaME in Algorithm 1 is given as follows. Given a randomly generated graph $G = ([m], E)$, extract neighbor sets $\{N_i : i \in [m]\}$. For each node $i \in [m]$, subset N_i^k is randomly selected from N_i such that $|N_i^k| = \lceil \nu_i |N_i| \rceil$. The parameters are initialized as follows: $\nu_i = \nu$, $s_i = s$, $\gamma_i = \gamma$, and $\sigma_i^0 = \sigma^0$ for all $i \in [m]$, where ν , s , γ , and σ^0 are specified in Table II unless stated otherwise. When analyzing the effect of a particular parameter, its value is adjusted and described explicitly. Moreover, for each node $i \in [m]$, integer κ_i is randomly selected from a predefined interval that varies across examples, as reported in Table II. Therefore, all nodes operate with distinct communication periods, resulting in a partially synchronized training regime, a more realistic training deployment. Finally, we terminate the algorithm if

$$\text{std} \{f(\boldsymbol{\varpi}^{k-2}), f(\boldsymbol{\varpi}^{k-1}), f(\boldsymbol{\varpi}^k)\} < 10^{-3},$$

where ‘std’ represents the standard deviation.

TABLE II: Choices of parameters.

	ν	s/n	γ	σ^0	κ_i
Example 1	0.2	0.2	1.005	1.0	[3,7]
Example 2	0.2	0.2	1.005	1.0	[3,7]
Example 3	0.5	0.1	1.001	5.0	[5,10]
Example 4	0.5	0.1	1.001	5.0	[5,10]

C. Self-Comparison of PaME

To assess the performance of the proposed algorithm PaME under different settings in Example 1, we conduct a comprehensive comparison in four dimensions: transmission rate s/n , participation rate ν , communication period κ_i , and graph connectivity $\max_i |N_i|$.

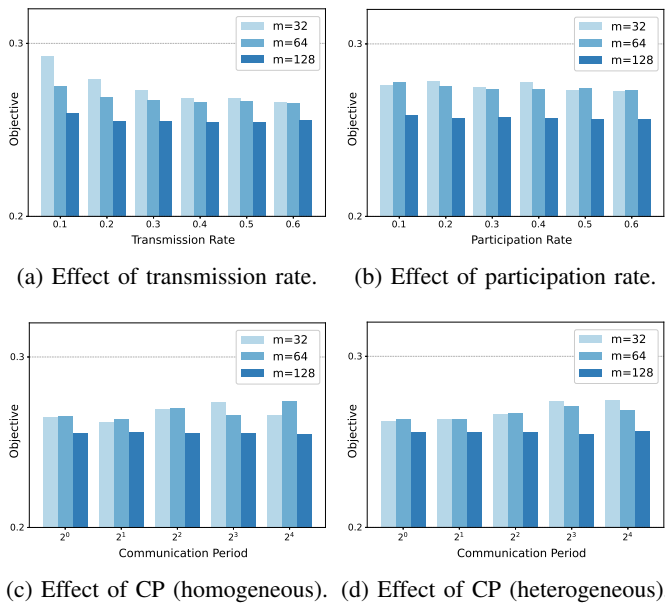


Fig. 2: Self-comparison of PaME.

1) *Effect of transmission rate:* Fig. 2a illustrates the effect of varying the transmission rate $s/n \in \{0.1, 0.2, \dots, 0.6\}$ across different numbers of nodes $m \in \{32, 64, 128\}$, with the participation rate fixed at $\nu = 0.2$. The results indicate that while higher transmission rates generally yield lower final objective values (i.e., improved accuracy), a high transmission rate is not strictly necessary. Notably, with a transmission rate of only 0.1, the final objective already approximates that obtained under full transmission. Furthermore, a larger number of nodes m tends to improve performance under low transmission rates. This is likely due to the fact that a larger m involves more participating nodes, thereby facilitating better information mixing. Based on the corresponding convergence curves in Fig. 3, the marginal gain becomes negligible once the rate exceeds approximately 0.2, although higher transmission rates accelerate convergence. This demonstrates that the proposed mechanism achieves satisfactory convergence while reducing communication costs by at least 80%.

2) *Effect of participation rate:* Fig. 2b illustrates the impact of varying participation rate $\nu \in \{0.1, 0.2, \dots, 0.6\}$ across different numbers of nodes $m \in \{32, 64, 128\}$, with the transmission rate fixed at $s/n = 0.2$. From the figure, while higher participation rates generally yield better model accuracy, the impact on the final objective value is relatively modest provided the rate is not extremely low; notably, all configurations eventually achieve convergence. The convergence trajectories in Fig. 4 further confirm that higher participation rates accelerate convergence. However, this improvement exhibits clear diminishing returns: increasing r from 0.1 to 0.2 significantly boosts convergence speed, whereas further increases yield only marginal gains. Given that higher participation implies a heavier communication load, these findings suggest the existence of a favorable trade-off point where a relatively low participation rate suffices for reasonably fast convergence.

3) *Effect of communication period (CP):* Fig. 2c and Fig. 2d illustrate the impact of the CP under homogeneous and het-

erogeneous settings. In the homogeneous setting, all nodes adopt a uniform period $\kappa_i = k_0 \in \{2^0, 2^1, \dots, 2^4\}$, whereas in the heterogeneous setting, nodes operate with distinct communication intervals whose median values correspond to those in the homogeneous case. The results indicate that the CP has minimal influence on the final objective value although larger periods in the heterogeneous setting may induce slight instability. The convergence trajectories in Fig. 5 and Fig. 6 further reveal that while shorter CPs generally accelerate convergence, this effect becomes less pronounced as the number of nodes m increases. Furthermore, heterogeneous CPs consistently yield slightly slower convergence than the homogeneous setting across all configurations.

4) *Effect of graph connectivity:* Fig. 7 examines the impact of graph connectivity by fixing the number of nodes to $m = 64$ and the participation rate to $\nu = 0.4$ while varying the transmission rate and the normalized graph degree (i.e., the maximum number of neighbors per node, normalized to $[0, 1]$). The three heatmaps report the final objective value, the number of iterations required for convergence, and the corresponding wall-clock time. The first heatmap indicates that increasing either s or the graph degree generally lowers the final objective, corresponding to improved model performance. Notably, unless the graph is extremely sparse or the transmission rate is minimal, the final objective quickly saturates and becomes nearly insensitive to further increases in either parameter. This suggests that PaME can achieve near-optimal performance even with a relatively low transmission rate, provided that the communication graph maintains moderate connectivity, thereby reinforcing its communication efficiency. The iteration and time heatmaps further corroborate this trend: except for the most challenging regime characterized by very sparse connectivity and small s , PaME demonstrates consistent convergence behavior (requiring approximately 200 iterations) and comparable runtime across a broad range of settings.

D. Comparison with other DFL algorithms

To further evaluate the performance of PaME, we benchmark it against four state-of-the-art baseline methods: D-PSGD [7] and DFedSAM [8], BEER [29], and ANQ-NIDS [32]. The latter two algorithms incorporate compression techniques to enhance communication efficiency. To ensure fair comparison, the communication period and participation rate are standardized across all methods.

5) *Comparison of convergence speed:* Fig. 8 presents the convergence curves for Example 2, with the number of nodes varying across $m \in \{32, 64, 128\}$ and the model dimension fixed at $n = 1000$. The results indicate that increasing m accelerates convergence. PaME consistently outperforms all competing algorithms in terms of convergence speed, requiring the fewest communication rounds to achieve the highest test accuracy. DFedSAM generally secures the second-best performance, whereas BEER and ANQ-NIDS exhibit slower convergence, likely due to information loss induced by compression.

6) *Comparison of communication efficiency:* Fig. 9 and Fig. 10 assess the communication efficiency for Example 2 when varying number of nodes $m \in \{32, 64, 128\}$ and model

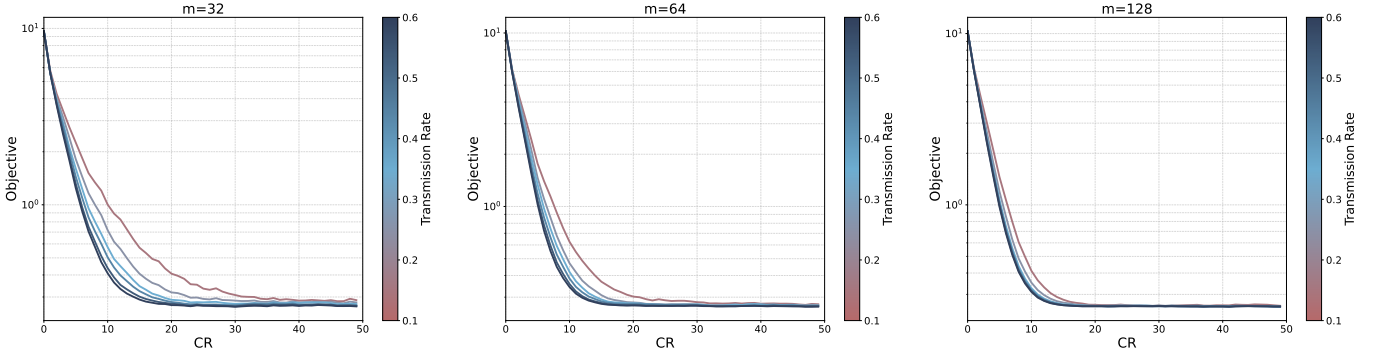


Fig. 3: Self comparison of PaME: Convergence curve of different transmission rate.

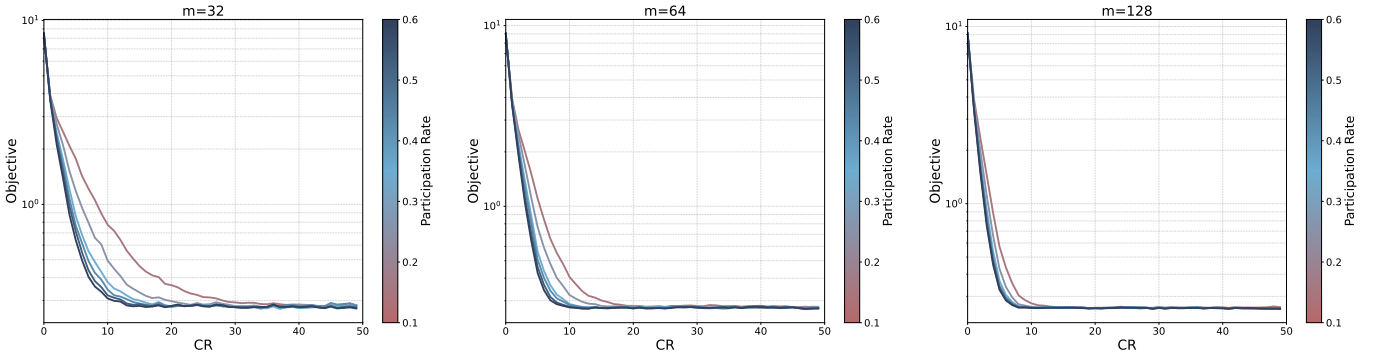


Fig. 4: Self comparison of PaME: Convergence curve of different participation rate.

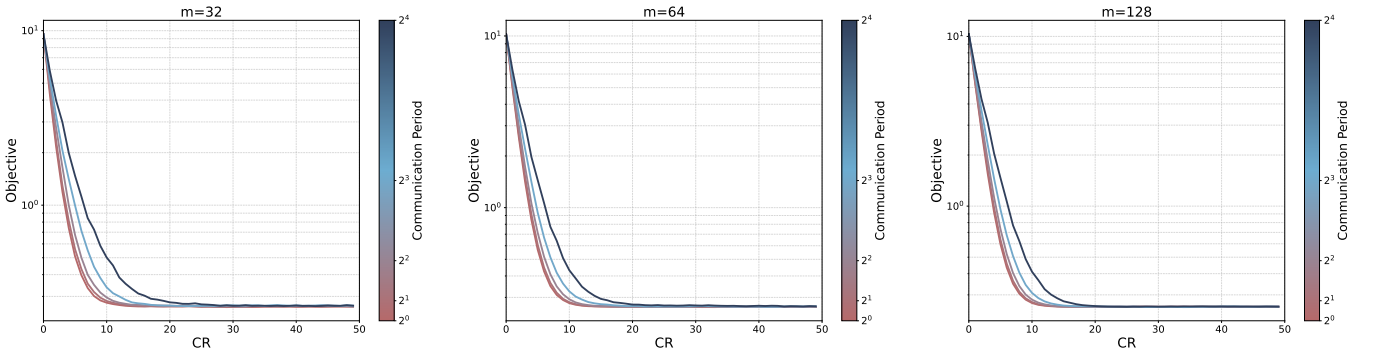


Fig. 5: Self comparison of PaME: Convergence curve of different CPs (homogeneous).

dimension $n \in \{1000, 5000, 10000\}$. Fig. 9 reports the number of communication rounds (CR) each algorithm needs to reach convergence, and PaME consistently requires the fewest CR across all configurations. Fig. 10 further compares the total data transmission volume required by each algorithm to reach convergence. Across all examined settings, PaME attains the lowest communication cost, typically reducing the transmitted volume by at least 50% compared with the other methods in most configurations. Together with the convergence results, these findings indicate that PaME achieves a more favorable trade-off between accuracy and communication efficiency.

7) *Comparison of data distribution*: Fig. 11 depicts the convergence trajectories for Example 3 under varying degrees of data heterogeneity, simulated by assigning each node samples from $C \in \{1, 7, 10\}$ distinct categories, where a lower value of C corresponds to a higher level of heterogeneity (non-IID). As expected, increased heterogeneity leads to performance

degradation across all evaluated methods. Nevertheless, PaME consistently maintains the fastest convergence speed across all scenarios. Notably, even under the most extreme setting (i.e., $C = 1$), PaME outperforms competing algorithms and achieves superior final accuracy.

Fig. 12 extends this analysis to Example 4 by comparing IID settings with Dirichlet partitions parameterized by $\beta \in \{0.3, 0.6\}$, where a lower β signifies higher data heterogeneity. The results indicate that PaME consistently outperforms other decentralized baselines. Although higher levels of non-IID data inherently complicate model consensus, PaME exhibits robust convergence stability and achieves the highest accuracy among the compared methods.

VI. CONCLUSION

This paper introduces PaME, a DFL algorithm to improve the trade-off among communication efficiency, privacy preser-

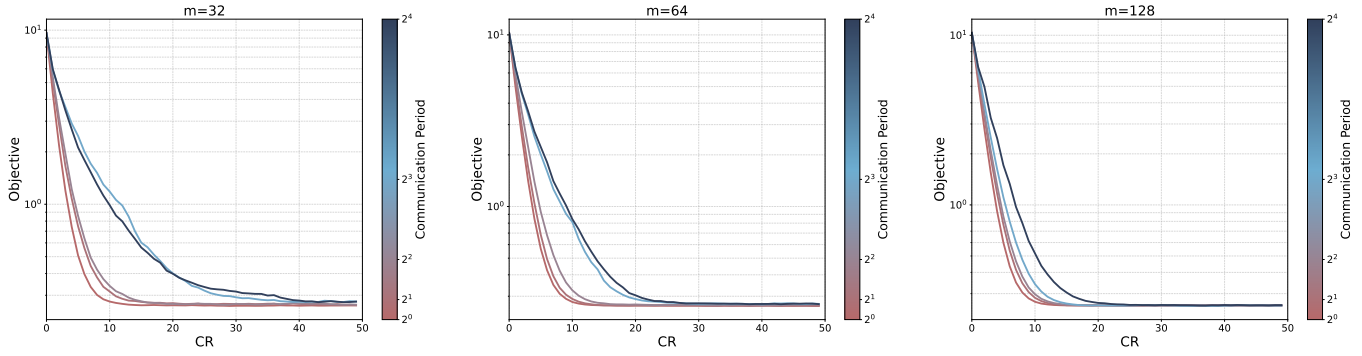


Fig. 6: Self-comparison of PaME: Convergence curve of different CPs (heterogeneous).

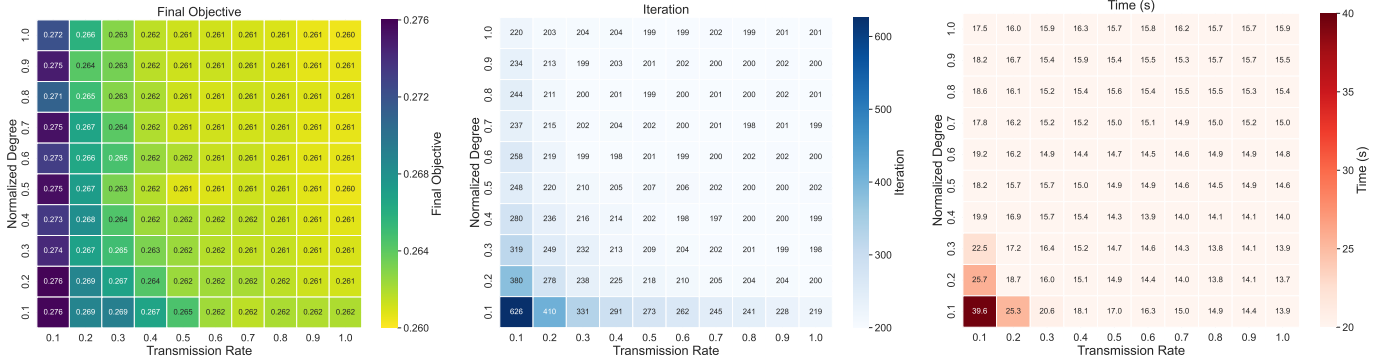


Fig. 7: Self-comparison of PaME: Heatmap of final objective, iteration, and runtime.

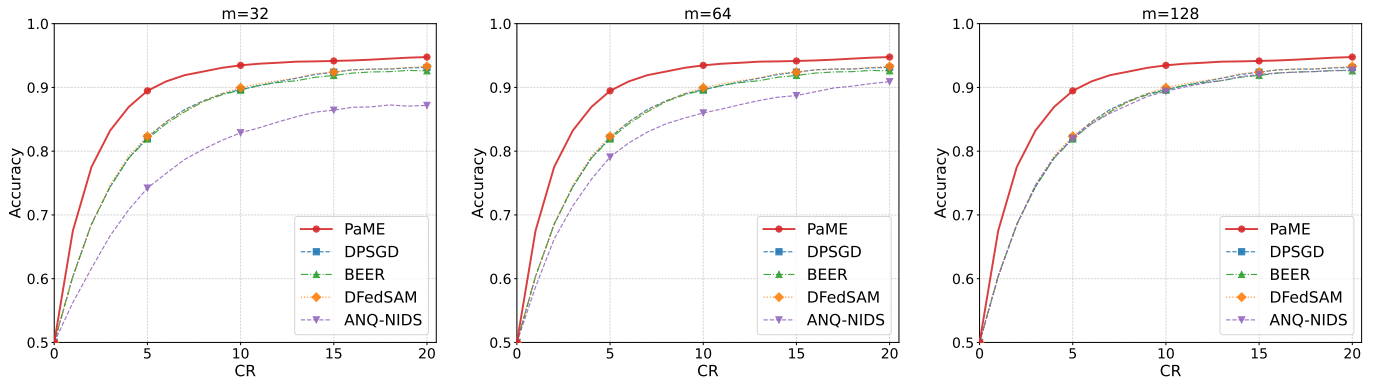


Fig. 8: Accuracy v.s. CR.

vation, and model utility. Its effectiveness stems from a novel partial message exchange mechanism, which is well suited to a variety of real-world scenarios, including unreliable wireless communications and edge computing environments. Moreover, rigorous theoretical guarantees are established under mild assumptions, which relax strict conditions significantly and thus enhance the robustness of DFL, particularly in the presence of heterogeneous data, highlighting strong potential of PaME for practical applications.

REFERENCES

[1] E. T. M. Beltrán, M. Q. Pérez, P. M. S. Sánchez, S. L. Bernal, G. Bovet, M. Gil, G. Martínez, and A. H. Celadrán, “Decentralized federated learning: Fundamentals, state of the art, frameworks, trends, and challenges,” *IEEE Commun. Surveys Tuts.*, 2023.

[2] E. Hallaji, R. Razavi-Far, M. Saif, B. Wang, and Q. Yang, “Decentralized federated learning: A survey on security and privacy,” *IEEE Trans. Big Data*, vol. 10, no. 2, pp. 194–213, 2024.

[3] M. Alabadi, A. Habbal, and M. Guizani, “An innovative decentralized and distributed deep learning framework for predictive maintenance in the industrial internet of things,” *IEEE Internet Things J.*, vol. 11, no. 11, pp. 20 271–20 286, 2024.

[4] P. Wang, H. Yang, G. Han, R. Yu, L. Yang, G. Sun, H. Qi, X. Wei, and Q. Zhang, “Decentralized navigation with heterogeneous federated reinforcement learning for uav-enabled mobile edge computing,” *IEEE Trans. Mobile*

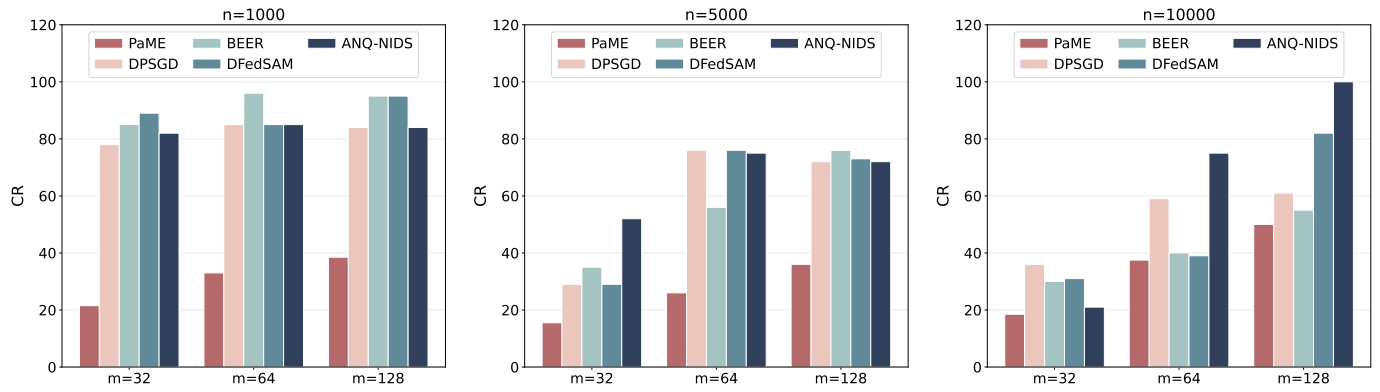


Fig. 9: CR v.s. m .

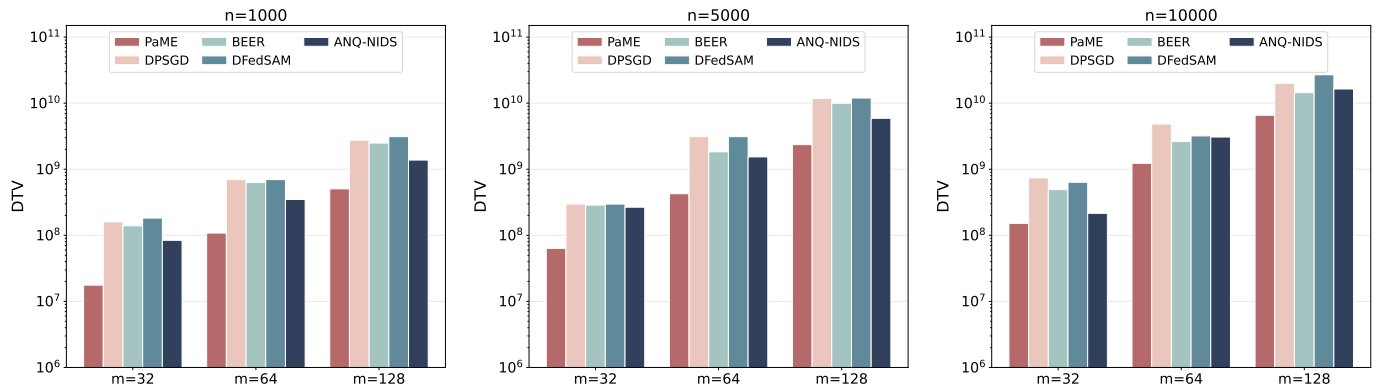


Fig. 10: Data transmission volume (DTV) v.s. m .

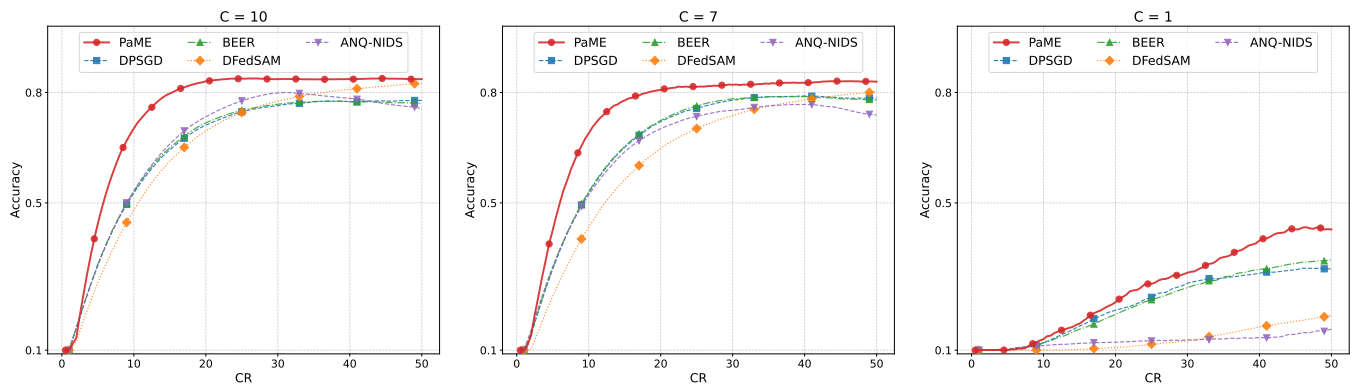


Fig. 11: Accuracy v.s. CR.

Comput., 2024.

[5] R. S. Nuvvula, P. P. Kumar, P. Akki, S. R. Ahammed, A. Ali *et al.*, “Federated learning-based energy forecasting and trading platform for decentralized renewable energy markets,” in *Int. Conf. Smart Grid. IEEE*, 2024, pp. 277–283.

[6] S. H. Alsamhi, R. Myrzasheva, A. Hawbani, S. Kumar, S. Srivastava, L. Zhao, X. Wei, M. Guizan, and E. Curry, “Federated learning meets blockchain in decentralized data sharing: Healthcare use case,” *IEEE Internet Things J.*, vol. 11, no. 11, pp. 19602–19615, 2024.

[7] X. Lian, C. Zhang, H. Zhang, C.-J. Hsieh, W. Zhang, and J. Liu, “Can decentralized algorithms outperform centralized algorithms? a case study for decentralized

parallel stochastic gradient descent,” *Adv. Neural Inf. Process. Syst.*, vol. 30, 2017.

[8] Y. Shi, L. Shen, K. Wei, Y. Sun, B. Yuan, X. Wang, and D. Tao, “Improving the model consistency of decentralized federated learning,” in *Proc. Int. Conf. Mach. Learn.*, 2023, pp. 31269–31291.

[9] T. Zhu, F. He, L. Zhang, Z. Niu, M. Song, and D. Tao, “Topology-aware generalization of decentralized sgd,” in *Proc. Int. Conf. Mach. Learn.*, 2022, pp. 27479–27503.

[10] C. Zhang, Q. Li, and P. Zhao, “Decentralized optimization with edge sampling,” in *Proc. Int. Joint Conf. Artif. Intell.*, 2019, pp. 658–664.

[11] M. De Vos, S. Farhadkhani, R. Guerraoui, A.-M. Kermarrec, R. Pires, and R. Sharma, “Epidemic learning:

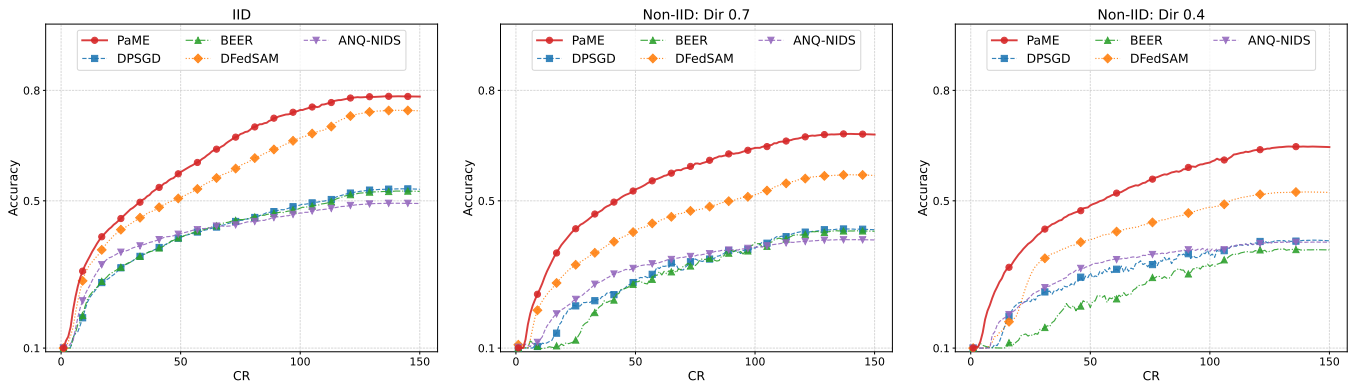


Fig. 12: Accuracy v.s. CR.

- Boosting decentralized learning with randomized communication,” *Adv. Neural Inf. Process. Syst.*, vol. 36, pp. 36 132–36 164, 2023.
- [12] L. Wang, Y. Chen, Y. Guo, and X. Tang, “Smart sampling: Helping from friendly neighbors for decentralized federated learning,” *arXiv preprint arXiv:2407.04460*, 2024.
- [13] A. Zhang, P. Zhao, W. Lu, and G. Zhang, “Personalized decentralized federated learning: A privacy-enhanced and byzantine-resilient approach,” *IEEE Trans. Comput. Social Syst.*, 2025.
- [14] A. Nedic and A. Ozdaglar, “Distributed subgradient methods for multi-agent optimization,” *IEEE Trans. Autom. Control*, vol. 54, no. 1, pp. 48–61, 2009.
- [15] H. Tang, S. Gan, C. Zhang, T. Zhang, and J. Liu, “Communication compression for decentralized training,” *Adv. Neural Inf. Process. Syst.*, vol. 31, 2018.
- [16] D. Alistarh, T. Hoefler, M. Johansson, N. Konstantinov, S. Khirirat, and C. Renggli, “The convergence of sparsified gradient methods,” *Adv. Neural Inf. Process. Syst.*, vol. 31, 2018.
- [17] S. Sha, S. Zhou, L. Kong, and G. Y. Li, “Sparse decentralized federated learning,” *IEEE Trans. Signal Process.*, vol. 73, pp. 3406–3420, 2025.
- [18] H. Ye, L. Liang, and G. Y. Li, “Decentralized learning with unreliable communications,” *IEEE J. Sel. Top. Signal Process*, vol. 16, no. 3, pp. 487–500, 2022.
- [19] X. Qian, H. Li, M. Hao, G. Xu, H. Wang, and Y. Fang, “Decentralized multi-client functional encryption for inner product with applications to federated learning,” *IEEE Trans. Depend. Sec. Comput.*, vol. 21, no. 6, pp. 5781–5796, 2024.
- [20] A. Saidi, A. Amira, and O. Nouali, “Securing decentralized federated learning: cryptographic mechanisms for privacy and trust,” *Cluster Comput.*, vol. 28, no. 2, p. 144, 2025.
- [21] Y. Wang and T. Başar, “Decentralized nonconvex optimization with guaranteed privacy and accuracy,” *Automatica*, vol. 150, p. 110858, 2023.
- [22] X.-Y. Yue, J.-W. Xiao, X.-K. Liu, and Y.-W. Wang, “Differentially private linearized admm algorithm for decentralized nonconvex optimization,” *IEEE Trans. Inf. Forensics Security*, 2025.
- [23] T. Fukami, T. Murata, K. Niwa, and I. Tyou, “Dp-norm: Differential privacy primal-dual algorithm for decentralized federated learning,” *IEEE Trans. Inf. Forensics Security*, vol. 19, pp. 5783–5797, 2024.
- [24] S. Zhou and G. Y. Li, “Federated learning via inexact admm,” *IEEE Trans. Pattern Anal. Mach. Intell.*, vol. 45, no. 8, pp. 9699–9708, 2023.
- [25] T. Sun, D. Li, and B. Wang, “Decentralized federated averaging,” *IEEE Trans. Pattern Anal. Mach. Intell.*, vol. 45, no. 4, pp. 4289–4301, 2022.
- [26] W. Liu, L. Chen, and W. Zhang, “Decentralized federated learning: Balancing communication and computing costs,” *IEEE Trans. Signal Inf. Process. Netw.*, vol. 8, pp. 131–143, 2022.
- [27] A. Koloskova, T. Lin, S. U. Stich, and M. Jaggi, “Decentralized deep learning with arbitrary communication compression,” in *Int. Conf. Learn. Represent.*, 2020.
- [28] N. Singh, D. Data, J. George, and S. Diggavi, “Squarmsgd: Communication-efficient momentum sgd for decentralized optimization,” *IEEE J. Sel. Areas Inf. Theory*, vol. 2, no. 3, pp. 954–969, 2021.
- [29] H. Zhao, B. Li, Z. Li, P. Richtárik, and Y. Chi, “Beer: Fast $o(1/t)$ rate for decentralized nonconvex optimization with communication compression,” *Adv. Neural Inf. Process. Syst.*, vol. 35, pp. 31 653–31 667, 2022.
- [30] Z. Liu and B. K. H. Low, “Decentralized sum-of-nonconvex optimization,” in *Proc. AAAI Conf. Artif. Intell.*, vol. 38, no. 13, 2024, pp. 14 088–14 096.
- [31] Z. Li, W. Shi, and M. Yan, “A decentralized proximal-gradient method with network independent step-sizes and separated convergence rates,” *IEEE Trans. Signal Process.*, vol. 67, no. 17, pp. 4494–4506, 2019.
- [32] N. Michelusi, G. Scutari, and C.-S. Lee, “Finite-bit quantization for distributed algorithms with linear convergence,” *IEEE Trans. Inf. Theory*, vol. 68, no. 11, pp. 7254–7280, 2022.
- [33] X. Zhang, M. Fang, J. Liu, and Z. Zhu, “Private and communication-efficient edge learning: A sparse differential gaussian-masking distributed sgd approach,” in *Int. Symp. Theory, Algorithmic Found., Protoc. Design Mobile Netw. Mobile Comput.*, 2020, pp. 261–270.

- [34] R. Hu, Y. Guo, and Y. Gong, “Federated learning with sparsified model perturbation: Improving accuracy under client-level differential privacy,” *IEEE Trans. Mobile Comput.*, vol. 23, no. 8, pp. 8242–8255, 2023.
- [35] S. Biswas, A.-M. Kermarrec, R. Pires, R. Sharma, and M. Vujasinovic, “Secure aggregation meets sparsification in decentralized learning,” *arXiv preprint arXiv:2405.07708*, 2024.
- [36] J. Nocedal, “Numerical optimization,” *Springer Ser. Oper. Res. Financ. Eng./Springer*, 2006.
- [37] S. Zheng, Q. Meng, T. Wang, W. Chen, N. Yu, Z. Ma, and T.-Y. Liu, “Asynchronous stochastic gradient descent with delay compensation for distributed deep learning,” *arXiv preprint arXiv:1609.08326*, 2016.
- [38] H. Yu, S. Yang, and S. Zhu, “Parallel restarted sgd with faster convergence and less communication: Demystifying why model averaging works for deep learning,” in *Proc. AAAI Conf. Artif. Intell.*, vol. 33, no. 1, 2019, pp. 5693–5700.
- [39] J. Wang and G. Joshi, “Cooperative sgd: A unified framework for the design and analysis of local-update sgd algorithms,” *J. Mach. Learn. Res.*, vol. 22, no. 213, pp. 1–50, 2021.
- [40] B. McMahan, E. Moore, D. Ramage, S. Hampson, and B. Aguera y Arcas, “Communication-efficient learning of deep networks from decentralized data,” in *Artif. Intell. Stat.*, 2017, pp. 1273–1282.
- [41] X. Li, K. Huang, W. Yang, S. Wang, and Z. Zhang, “On the convergence of fedavg on non-iid data,” *arXiv preprint arXiv:1907.02189*, 2019.
- [42] T. Li, A. K. Sahu, M. Zaheer, M. Sanjabi, A. Talwalkar, and V. Smith, “Federated optimization in heterogeneous networks,” *Proc. Mach. Learn. Syst.*, vol. 2, pp. 429–450, 2020.
- [43] S. Zhou and G. Y. Li, “Fedgia: An efficient hybrid algorithm for federated learning,” *IEEE Trans. Signal Process.*, vol. 71, pp. 1493–1508, 2023.
- [44] H. Kaplan, Y. Mansour, and U. Stemmer, “The sparse vector technique, revisited,” in *Conf. Learn. Theory (COLT)*, 2021, pp. 2747–2776.
- [45] Y. Zhu and Y.-X. Wang, “Improving sparse vector technique with renyi differential privacy,” *Adv. Neural Inf. Process. Syst.*, vol. 33, pp. 20 249–20 258, 2020.
- [46] Y. Li, T.-H. Chang, and C.-Y. Chi, “Secure federated averaging algorithm with differential privacy,” in *IEEE Int. Workshop Mach. Learn. Signal Process.* IEEE, 2020, pp. 1–6.
- [47] Y. Li, S. Wang, T.-H. Chang, and C.-Y. Chi, “Federated stochastic primal-dual learning with differential privacy,” *arXiv preprint arXiv:2204.12284*, 2022.
- [48] H. Xiao, K. Rasul, and R. Vollgraf, “Fashion-mnist: a novel image dataset for benchmarking machine learning algorithms,” *arXiv preprint arXiv:1708.07747*, 2017.
- [49] K. He, X. Zhang, S. Ren, and J. Sun, “Deep residual learning for image recognition,” in *Proc. IEEE Conf. Comput. Vis. Pattern Recognit.*, 2016, pp. 770–778.
- [50] A. Krizhevsky, G. Hinton *et al.*, “Learning multiple layers of features from tiny images,” 2009.



Shan Sha received the B.S. degree from the School of Mathematics and Statistics, Beijing Jiaotong University, Beijing, China, in 2019, where she is currently working toward the PhD degree. From 2023 to 2024, she was a visiting Ph.D. student with the Intelligent Transmission and Processing Lab in Imperial College London. Her research interests include optimization theory and algorithms for federated learning.



Shenglong Zhou received the Ph.D. degree from the University of Southampton, Southampton, U.K., in 2018, where he was a Research Fellow and a Teaching Fellow. From 2021 to 2023, he was a Research Fellow with Imperial College London, London, U.K. He is currently a Professor with Beijing Jiaotong University, Beijing, China. His research interests include the theory and methods for optimization in the areas of sparse, low-rank matrix, 0/1 loss, and machine learning-related optimization.



Xin Wang is a Lecturer at Beijing Jiaotong University, Beijing, China. He received his Ph.D. degree from the School of Mathematics and Statistics, Beijing Jiaotong University. His research interests include high-dimensional statistical analysis, optimization theory and algorithms.



Lingchen Kong received the Ph.D. degree from the School of Science, Beijing Jiaotong University, Beijing, China, in 2007. He is currently a professor of School of Mathematics and Statistics at Beijing Jiaotong University, Beijing, China. He was a Visiting Scholar with the Department of Statistics, University of Minnesota, Twin Cities, USA, from 2014 to 2015. His research interests include the large scale optimization, sparse optimization, linear regression, matrix regression, clustering, high-dimensional statistical analysis, etc.



Geoffrey Ye Li is currently a Chair Professor at Imperial College London, UK. Before joining Imperial in 2020, he was a Professor at Georgia Institute of Technology for 20 years and a Principal Technical Staff Member with AT&T Labs – Research (previous Bell Labs) for five years. He made fundamental contributions to orthogonal frequency division multiplexing (OFDM) for wireless communications, established a framework on resource cooperation in wireless networks, and introduced deep learning to communications. In these areas, he has published

over 700 journal and conference papers in addition to over 40 granted patents. His publications have been cited over 80,000 times with an H-index over 130. He has been listed as a Highly Cited Researcher by Clarivate/Web of Science almost every year.

Dr. Geoffrey Ye Li was elected to Fellow of the Royal Academic of Engineering (FREng), IEEE Fellow, and IET Fellow for his contributions to signal processing for wireless communications. He received 2024 IEEE Eric E. Sumner Award, 2019 IEEE ComSoc Edwin Howard Armstrong Achievement Award, and several other awards from IEEE Signal Processing, Vehicular Technology, and Communications Societies.

Supplemental Material for "Decentralized Federated Learning by Partial Message Exchange"

Shan Sha, Shenglong Zhou, Xin Wang, Lingchen Kong, Geoffrey Ye Li, *IEEE Fellow*

I. Proof Theorem 1

Theorem 1. Let $\bar{\mathbf{w}}$ be the average of q vectors $\mathbf{w}_1, \mathbf{w}_2, \dots, \mathbf{w}_q \in \mathbb{R}^n$. For each $i \in [q]$, independently construct a sparse vector $\mathbf{v}_i \in \mathbb{R}^n$ by uniformly selecting s coordinates of \mathbf{w}_i without replacement from $[q]$. Define indicator variables by

$$\delta_{i\ell} = \begin{cases} 1, & \text{if } w_{i\ell} \text{ is selected,} \\ 0, & \text{otherwise,} \end{cases} \quad \delta_\ell := \sum_{i=1}^q \delta_{i\ell}.$$

and two averages $\bar{\mathbf{v}}$ and $\tilde{\mathbf{v}}$ by

$$\bar{v}_\ell = \begin{cases} \frac{1}{\delta_\ell} \sum_{i=1}^q v_{i\ell}, & \text{if } \delta_\ell > 0, \\ 0, & \text{otherwise,} \end{cases} \quad \tilde{v}_\ell = \frac{1}{q} \sum_{i=1}^q v_{i\ell}$$

for any $\ell \in [n]$. Then

$$\mathbb{E}(\bar{v}_\ell \mid \delta_\ell > 0) = \bar{w}_\ell, \quad \mathbb{E}(\tilde{v}_\ell \mid \delta_\ell > 0) = \frac{s}{n} \bar{w}_\ell. \quad (1)$$

Proof. The definition of $\delta_{i\ell}$ and construction of \mathbf{v}_i implies that when $\delta_\ell > 0$ it follows

$$\bar{v}_\ell = \frac{1}{\delta_\ell} \sum_{i=1}^q v_{i\ell} = \frac{1}{\delta_\ell} \sum_{i=1}^q \delta_{i\ell} w_{i\ell}.$$

Given $\delta_\ell = k > 0$, exactly k indices among $[q]$ satisfy $\delta_{i\ell} = 1$. Since the selections for different vectors are independent and symmetric, conditioning on $\delta_\ell = k$ implies that these k indices form a uniformly random subset of $[q]$ of size k . Therefore,

$$\mathbb{E}(\bar{v}_\ell \mid \delta_\ell = k) = \frac{1}{k} \mathbb{E} \sum_{i: \delta_{i\ell}=1} w_{i\ell} = \frac{1}{k} \frac{k}{q} \sum_{i=1}^q w_{i\ell} = \bar{w}_\ell.$$

Since the above expectation does not depend on k , taking expectation over $\delta_\ell > 0$ yields the first equation in (1).

By the definition of $\delta_{i\ell}$ and construction of \mathbf{v}_i ,

$$\tilde{v}_\ell = \frac{1}{q} \sum_{i=1}^q v_{i\ell} = \frac{1}{q} \sum_{i=1}^q \delta_{i\ell} w_{i\ell}.$$

For each $i \in [q]$, since s coordinates are selected uniformly from $[n]$, it holds $\mathbb{P}(\delta_{i\ell} = 1) = s/n$. This immediately results in $\mathbb{E}(\delta_{i\ell} w_{i\ell}) = s w_{i\ell}/n$, and consequently,

$$\mathbb{E}(\tilde{v}_\ell) = \frac{1}{q} \sum_{i=1}^q \frac{s}{n} w_{i\ell} = \frac{s}{n} \bar{w}_\ell.$$

Conditioning on $\{\delta_\ell > 0\}$ does not affect this expectation, since \tilde{v}_ℓ is linear in $\delta_{i\ell}$ and the conditional expectation remains unchanged. Hence, the second equation in (1) holds. \square

II. Algorithm, Assumption, and Setup

Assumption 1. Suppose network matrix \mathbf{B} is a doubly stochastic matrix satisfying

$$\zeta := \max\{|\lambda_2(\mathbf{B})|, |\lambda_m(\mathbf{B})|\} < 1. \quad (6)$$

where $\lambda_i(\mathbf{B})$ is the i th largest eigenvalue of \mathbf{B} and \mathbf{B} is defined by by

$$B_{ji} := \begin{cases} \frac{1}{m_i}, & \text{if } j \in N_i, \\ 0, & \text{otherwise,} \end{cases} \quad (7)$$

Note that doubly stochastic matrix satisfies

$$\mathbf{B}\mathbf{1}^\top = \mathbf{1}^\top \mathbf{B} = \mathbf{1}^\top, \quad \mathbf{J}\mathbf{B} = \mathbf{B}\mathbf{J} = \mathbf{J}, \quad \text{with } \mathbf{J} := \frac{\mathbf{1}\mathbf{1}^\top}{m}, \quad (8)$$

Algorithm 1 DFL by Partial Message Exchange (PaME)

- 1: Initialize $\mathbf{w}_i^0 = \mathbf{0}$, two integers $\kappa_i > 0$ and $s_i > 0$, $\sigma_i^0 > 0$, $\gamma_i > 1$ for each $i \in [m]$.
- 2: **for** iteration $k = 0, 1, 2, 3, \dots$ **do**
- 3: **for** node $i = 1, 2, \dots, m$ **do**
- 4: **if** $k \in \mathcal{K}_i := \{0, \kappa_i, 2\kappa_i, 3\kappa_i, \dots\}$ **then**
- 5: Random neighbor selection: $N_i^k \subseteq N_i$.
- 6: Neighbor number update: $m_i^k = |N_i^k|$.
- 7: Partial message exchange: $\bar{\mathbf{v}}_i^k = \text{PME}(\mathbf{w}_i^k, \{\mathbf{w}_j^k : j \in N_i^k\})$.
- 8: **else**
- 9: Local parameter tracking: $\bar{\mathbf{v}}_i^k = \mathbf{w}_i^k$.
- 10: Neighbor number tracking: $m_i^k = m_i^{k-1}$.
- 11: **end if**
- 12: Random sub-batch data sampling: $\mathcal{B}_i^k \subseteq \mathcal{D}_i$.
- 13: Local parameter updating:

$$\mathbf{w}_i^{k+1} = \bar{\mathbf{v}}_i^k - \frac{\nabla f_i(\bar{\mathbf{v}}_i^k; \mathcal{B}_i^k)}{\sigma_i^k m_i^k}. \quad (2)$$

- 14: Hyper-parameter increasing: $\sigma_i^{k+1} = \gamma_i \sigma_i^k$.
 - 15: **end for**
 - 16: **end for**
-

Algorithm 2 $\bar{\mathbf{v}}_i^k = \text{PME}(\mathbf{w}_i^k, \{\mathbf{w}_j^k : j \in N_i^k\})$

- 1: **for** every node $j \in N_i^k$ **do**
- 2: Random subset selection: $T_j^k \subseteq [n]$ with $|T_j^k| = s_j$.
- 3: Sparse vector \mathbf{v}_j^k generation:

$$v_{j\ell}^k = \begin{cases} w_{j\ell}^k, & \text{if } \ell \in T_j^k, \\ 0, & \text{if } \ell \notin T_j^k. \end{cases} \quad (3)$$

- 4: Partial message \mathbf{v}_j^k exchange to node i .
- 5: **end for**
- 6: Node i averages received messages by

$$\bar{v}_{i\ell}^k = \begin{cases} \frac{\sum_{j \in N_i^k} v_{j\ell}^k}{\lambda_{i,\ell}^k}, & \text{if } \lambda_{i,\ell}^k \neq 0, \\ w_{i\ell}^k, & \text{if } \lambda_{i,\ell}^k = 0, \end{cases} \quad (4)$$

for each $\ell \in [n]$, where

$$\lambda_{i,\ell}^k = |\{j \in N_i^k : v_{j\ell}^k \neq 0\}|. \quad (5)$$

where $\mathbf{1}$ be a vector with all entries being 1. It is easy to see that \mathbf{B} satisfies

$$\|\mathbf{B} - \mathbf{J}\|_2^2 \leq \zeta^2, \quad \|\mathbf{I} - \mathbf{B}\|_2^2 \leq (\|\mathbf{I} - \mathbf{J}\| + \|\mathbf{B} - \mathbf{J}\|)^2 \leq (1 + \zeta)^2. \quad (9)$$

Assumption 2. For each $i \in [m]$, ∇f_i is Lipschitz continuous with $\alpha_i > 0$ on $\mathbb{N}(2\delta)$ for a given $\delta \in (0, \infty)$, where

$$\mathbb{N}(2\delta) := \{\mathbf{w} \in \mathbb{R}^n : \|\mathbf{w}\|_\infty \leq 2\delta\}$$

and $\|\mathbf{w}\|_\infty$ denotes the infinity norm of \mathbf{w} .

Setup 1. Parameters in Algorithm 1 are chosen as follows.

- 1) Set $\mathbf{W}^0 = \mathbf{0}$ and $\kappa_i = k_0$ for all $i \in [m]$. This is adopted for analytical convenience without loss of generality. In fact, one can always let k_0 be the least common multiple of $\{\kappa_1, \kappa_2, \dots, \kappa_m\}$, then the subsequent analysis remains similar to the case of $\kappa_i = k_0$.
- 2) Set $m_i^k = t_i = \lfloor \nu_i |N_i| \rfloor$ for all $k \geq 0$ and $i \in [m]$, where $\nu_i \in (0, 1]$ is the participation rate and $\lfloor a \rfloor$ is the floor of a . That is, at every iteration, node i selects the same number of neighbor nodes to join in the training.
- 3) Set $\sigma_i^0 = \sigma^0$ and $\gamma_i = \gamma$, $s_i = s$ for all $i \in [m]$. Again, this is adopted for analytical convenience without loss of generality. In fact, for different σ_i^0 and γ_i , we can conduct similar analysis by considering

$$\sigma^0 = \min\{\sigma_1^0, \dots, \sigma_m^0\}, \quad \gamma = \min\{\gamma_1, \dots, \gamma_m\}, \quad s = \min\{s_1, \dots, s_m\}.$$

Moreover, in Algorithm 2, each node $j \in N_i^k$ independently constructs a set T_j^k by uniformly selecting s entries of $[n]$ without replacement.

4) In the sequel, given $\zeta \in (0, 1)$ defined in (6) and integers k_0 and (t_1, \dots, t_m) , initialize

$$p := \frac{s}{n} \in (0, 1), \quad \gamma \in \left(1, \zeta^{-2/k_0}\right), \quad \nu_i \in (0, 1], \quad \forall i \in [m], \quad (10)$$

to satisfy

$$(1-p)^{t_i} (1+\zeta)^2 + 2p \sum_{j \in N_i} \nu_j < \left(\frac{1}{\gamma^{k_0/2}} - \zeta\right)^2, \quad \forall i \in [m]. \quad (11)$$

Moreover, define a useful constant by

$$\varepsilon_i(t) := \sup \left\{ \|\nabla f_i(\mathbf{w}; \mathcal{B}_i) - \nabla f_i(\mathbf{w}; \mathcal{B}'_i)\|_\infty : \mathcal{B}_i, \mathcal{B}'_i \subseteq \mathcal{D}_i, \mathbf{w} \in \mathbb{N}(t) \right\}, \quad \forall i \in [m]. \quad (12)$$

It is easy to see that such a constant $\varepsilon_i(t)$ is well defined for any given $t \in (0, \infty)$, namely,

$$0 < \varepsilon_i(t) < \infty \quad \text{for any given } t \in (0, \infty).$$

Based on this constant, we always choose σ^0 such that

$$\sigma^0 \geq \sigma := \max \left\{ 4\alpha_{\max}, \frac{\varepsilon(2\delta)\gamma}{(\gamma-1)\delta t_{\min}} \right\}, \quad (13)$$

where

$$\begin{aligned} \varepsilon(2\delta) &:= \max \left\{ \varepsilon_1(2\delta), \varepsilon_2(2\delta), \dots, \varepsilon_m(2\delta) \right\}, \\ \alpha_{\max} &:= \max \left\{ \alpha_1, \alpha_2, \dots, \alpha_m \right\}, \\ t_{\min} &:= \min \left\{ t_1, t_2, \dots, t_m \right\}. \end{aligned} \quad (14)$$

According to Setup 1, $\sigma_i^0 = \sigma^0$ and $\gamma_i = \gamma$ for all $i \in [m]$, one has

$$\sigma_i^{k+1} = \gamma_i \sigma_i^k = \gamma \sigma_i^k = \gamma^{k+1} \sigma_i^0 = \gamma^{k+1} \sigma^0.$$

As a consequence,

$$\sigma^k := \sigma_1^k = \dots = \sigma_m^k = \gamma \sigma^k = \gamma^k \sigma^0, \quad (15)$$

which results in

$$\sigma^{k+1} > \sigma^0 \geq \sigma = \max \left\{ 4\alpha_{\max}, \frac{\varepsilon(2\delta)\gamma}{(\gamma-1)\delta t_{\min}} \right\}. \quad (16)$$

Under Assumption 2 and (16), for $\forall i \in [m]$ and $\forall k \geq 0$,

$$\begin{aligned} f_i(\mathbf{w}) - f_i(\mathbf{v}) &\leq \langle \nabla f_i(\mathbf{u}), \mathbf{w} - \mathbf{v} \rangle + \frac{\alpha_i}{2} \|\mathbf{w} - \mathbf{v}\|^2 \\ &\stackrel{(16)}{\leq} \langle \nabla f_i(\mathbf{u}), \mathbf{w} - \mathbf{v} \rangle + \frac{\sigma^k}{8} \|\mathbf{w} - \mathbf{v}\|^2, \end{aligned} \quad (17)$$

where $\mathbf{u} = \mathbf{w}$ or $\mathbf{u} = \mathbf{v}$. Finally, recall that $f(\mathbf{w}) := \sum_{i=1}^m f_i(\mathbf{w})$ and each $f_i : \mathbb{R}^n \rightarrow \mathbb{R}$ is bounded from below. Denote

$$f^* := \sum_{i=1}^m f_i^{\min}, \quad \text{with } f_i^{\min} = \min_{\mathbf{w}} f_i(\mathbf{w}). \quad (18)$$

It is easy to see that $f^* \leq \min_{\mathbf{w}} \sum_{i=1}^m f_i(\mathbf{w})$.

III. Proofs of Theorems in Section III

A. Some Facts

First, let $\mathbb{I}(\cdot)$ be an indicator function defined by

$$\mathbb{I}(j \in N) = \begin{cases} 1, & \text{it } j \in N, \\ 0, & \text{it } j \notin N. \end{cases} \quad (19)$$

By Setup 1, there is $\kappa_i = k_0, \forall i \in [m]$. We use this k_0 to define

$$\mathcal{K}_0 := \{0, k_0, 2k_0, \dots\}. \quad (20)$$

According to (2) in Algorithm 1, for $\forall i \in [m]$,

$$\mathbf{w}_i^{k+1} = \bar{\mathbf{v}}_i^k - \mathbf{h}_i^k, \quad \bar{\mathbf{v}}_i^k = \begin{cases} \text{PME}(\mathbf{w}_i^k, \{\mathbf{w}_j^k : j \in N_i^k\}), & \text{when } k \in \mathcal{K}_0, \\ \mathbf{w}_i^k, & \text{when } k \notin \mathcal{K}_0, \end{cases} \quad (21)$$

where

$$\mathbf{h}_i^k := \frac{\mathbf{g}_i^k}{\sigma^k t_i}, \quad \mathbf{g}_i^k = \nabla f(\bar{\mathbf{v}}_i^k; \mathcal{B}_i^k). \quad (22)$$

For compactness, define a diagonal stepsize matrix and a stacked gradient matrix by

$$\mathbf{D}^k := \begin{bmatrix} \frac{1}{\sigma^k t_1} & 0 & \cdots & 0 \\ 0 & \frac{1}{\sigma^k t_2} & \cdots & 0 \\ \vdots & \vdots & \ddots & \vdots \\ 0 & 0 & \cdots & \frac{1}{\sigma^k t_m} \end{bmatrix}, \quad \mathbf{G}^k := (\mathbf{g}_1^k, \mathbf{g}_2^k, \dots, \mathbf{g}_m^k), \quad (23)$$

so that

$$\mathbf{H}^k := (\mathbf{h}_1^k, \dots, \mathbf{h}_m^k) = \mathbf{G}^k \mathbf{D}^k. \quad (24)$$

Letting $m_i = |N_i|$ and $t_i = |N_i^k|$, we denote three average points by

$$\boldsymbol{\varpi}^k := \frac{1}{m} \sum_{i=1}^m \mathbf{w}_i^k, \quad \widehat{\mathbf{w}}_i^k := \frac{1}{m_i} \sum_{j \in N_i} \mathbf{w}_j^k, \quad \widetilde{\mathbf{w}}_i^k := \frac{1}{t_i} \sum_{j \in N_i^k} \mathbf{w}_j^k, \quad (25)$$

which enable us to denote several matrices used in the sequel,

$$\begin{aligned} \boldsymbol{\Pi}^k &:= (\boldsymbol{\varpi}^k, \boldsymbol{\varpi}^k, \dots, \boldsymbol{\varpi}^k) = \mathbf{W}^k \mathbf{J}, \\ \mathbf{W}^k &:= (\mathbf{w}_1^k, \mathbf{w}_2^k, \dots, \mathbf{w}_m^k), \\ \mathbf{V}^k &:= (\bar{\mathbf{v}}_1^k, \bar{\mathbf{v}}_2^k, \dots, \bar{\mathbf{v}}_m^k), \\ \mathbf{W}^k \mathbf{B} &= (\widehat{\mathbf{w}}_1^k, \widehat{\mathbf{w}}_2^k, \dots, \widehat{\mathbf{w}}_m^k), \\ \mathbf{P}^k &:= \mathbf{V}^k - \mathbf{W}^k \mathbf{B}. \end{aligned} \quad (26)$$

This first condition in (26) leads to

$$\boldsymbol{\Pi}^k (\mathbf{B} - \mathbf{I}) = \mathbf{W}^k \mathbf{J} (\mathbf{B} - \mathbf{I}) \stackrel{(8)}{=} 0, \quad \boldsymbol{\Pi}^k (\mathbf{B} - \mathbf{J}) = \mathbf{W}^k \mathbf{J} (\mathbf{B} - \mathbf{J}) \stackrel{(8)}{=} 0. \quad (27)$$

Now, equation (21) implies the matrix recursion

$$\mathbf{W}^{k+1} = \mathbf{V}^k - \mathbf{H}^k = \mathbf{W}^k \mathbf{B} - \mathbf{H}^k + \mathbf{P}^k. \quad (28)$$

Finally, for any $\mathbf{w}_i, i \in [m]$, and $p > 0$ we have

$$\begin{aligned} 2\langle \mathbf{w}_1, \mathbf{w}_2 \rangle &\leq p \|\mathbf{w}_1\|^2 + \frac{1}{p} \|\mathbf{w}_2\|^2, \quad \|\mathbf{w}_1 + \mathbf{w}_2\|^2 \leq (1+p) \|\mathbf{w}_1\|^2 + \left(1 + \frac{1}{p}\right) \|\mathbf{w}_2\|^2, \\ \left\| \sum_{i=1}^m \mathbf{w}_i \right\| &\leq \sum_{i=1}^m \|\mathbf{w}_i\|, \quad \left\| \sum_{i=1}^m \mathbf{w}_i \right\|^2 \leq m \sum_{i=1}^m \|\mathbf{w}_i\|^2. \end{aligned} \quad (29)$$

B. Key Lemmas

Lemma 1. *Given an integer $\ell \geq 1$ and $x_1, \dots, x_\ell \in \mathbb{R}$ be arbitrary scalars. Let S be a uniformly random subset of $\{1, \dots, \ell\}$ without replacement and with size $|S| = \lambda$. Conditioned on the event $\lambda = r$ (where $1 \leq r \leq \ell$), we have*

$$\mathbb{E} \left[\left(\frac{1}{r} \sum_{j \in S} x_j \right)^2 \mid \lambda = r \right] \leq \frac{1}{\ell} \sum_{j=1}^{\ell} x_j^2. \quad (30)$$

Moreover, letting $\bar{x} := \frac{1}{\ell} \sum_{j=1}^{\ell} x_j$ and $\hat{x} := \frac{1}{r} \sum_{j \in S} x_j$, the variance formula for simple random sampling without replacement (SRSWOR) gives

$$\text{Var}(\hat{x} \mid \lambda = r) = \mathbb{E} \left[(\hat{x} - \bar{x})^2 \mid \lambda = r \right] = \frac{\ell - r}{r \ell (\ell - 1)} \sum_{j=1}^{\ell} (x_j - \bar{x})^2. \quad (31)$$

Proof. By Jensen's inequality,

$$\left(\frac{1}{r} \sum_{j \in S} x_j \right)^2 \leq \frac{1}{r} \sum_{j \in S} x_j^2.$$

Taking conditional expectation over the random subset S yields:

$$\mathbb{E} \left[\left(\frac{1}{r} \sum_{j \in S} x_j \right)^2 \mid \lambda = r \right] \leq \frac{1}{r} \sum_{j=1}^{\ell} \mathbb{P}(j \in S \mid \lambda = r) x_j^2 = \frac{1}{r} \sum_{j=1}^{\ell} \frac{r}{\ell} x_j^2 = \frac{1}{\ell} \sum_{j=1}^{\ell} x_j^2.$$

This shows (30). Since S is a simple random sample of size r drawn uniformly without replacement from $\{1, \dots, \ell\}$. Let

$$I_j := \begin{cases} 1, & \text{if } j \text{ is selected,} \\ 0, & \text{otherwise.} \end{cases}$$

Then $\hat{x} = \frac{1}{r} \sum_{j=1}^{\ell} I_j x_j$ and $\mathbb{E}[I_j \mid \lambda = r] = \frac{r}{\ell}$, which indicates that for $j \neq k$,

$$\mathbb{E}[I_j I_k \mid \lambda = r] = \frac{\binom{\ell-2}{r-2}}{\binom{\ell}{r}} = \frac{r(r-1)}{\ell(\ell-1)}.$$

Expanding the second moment gives

$$\begin{aligned} \mathbb{E}[\hat{x}^2 \mid \lambda = r] &= \frac{1}{r^2} \left(\sum_{j=1}^{\ell} \mathbb{E}[I_j \mid \lambda = r] x_j^2 + \sum_{j \neq k} \mathbb{E}[I_j I_k \mid \lambda = r] x_j x_k \right) \\ &= \frac{1}{r^2} \left(\frac{r}{\ell} \sum_{j=1}^{\ell} x_j^2 + \frac{r(r-1)}{\ell(\ell-1)} \sum_{j \neq k} x_j x_k \right) \\ &= \frac{1}{r^2} \left(\frac{r}{\ell} \sum_{j=1}^{\ell} x_j^2 + \frac{r(r-1)}{\ell(\ell-1)} \left(\ell^2 \bar{x}^2 - \sum_{j=1}^{\ell} x_j^2 \right) \right) \\ &= \frac{1}{r^2} \left(\frac{r(\ell-r)}{\ell(\ell-1)} \sum_{j=1}^{\ell} x_j^2 + \frac{r\ell(r-1)}{\ell-1} \bar{x}^2 \right) \\ &= \bar{x}^2 + \frac{\ell-r}{r\ell(\ell-1)} \left(\sum_{j=1}^{\ell} x_j^2 - \ell \bar{x}^2 \right) \\ &= \bar{x}^2 + \frac{\ell-r}{r\ell(\ell-1)} \sum_{j=1}^{\ell} (x_j - \bar{x})^2, \end{aligned}$$

where the third equation is from

$$\sum_{j \neq k} x_j x_k = \left(\sum_{j=1}^{\ell} x_j \right)^2 - \sum_{j=1}^{\ell} x_j^2 = \ell^2 \bar{x}^2 - \sum_{j=1}^{\ell} x_j^2.$$

The above condition and $\mathbb{E}[\hat{x} \mid \lambda = r] = \bar{x}$ from (1) imply $\text{Var}(\hat{x} \mid \lambda = r) = \mathbb{E}[(\hat{x} - \bar{x})^2 \mid \lambda = r]$ and yield (31). \square

Lemma 2. Let $\{(\mathbf{W}^k, \mathbf{V}^k)\}$ be the sequence generated by Algorithm 1 with Setup 1. Then for any $k \geq 1$,

$$\begin{aligned} \sum_{i=1}^m 2t_i \mathbb{E} \|\mathbf{w}_i^k - \bar{\mathbf{v}}_i^k\|^2 &\leq 8m \mathbb{E} \|\mathbf{W}^k - \mathbf{\Pi}^k\|_F^2, \\ \mathbb{E} \|\mathbf{W}^k - \mathbf{V}^k\|_F^2 &\leq \frac{4m}{t_{\min}} \mathbb{E} \|\mathbf{W}^k - \mathbf{\Pi}^k\|_F^2. \end{aligned} \tag{32}$$

Proof. We proof the result by considering two cases.

Case 1: $k \notin \mathcal{K}_0$. Under such a case, Algorithm 1 states that $\bar{\mathbf{v}}_i^k = \mathbf{w}_i^k$ for any $i \in [m]$. Therefore, (32) holds clearly.

Case 2: $k \in \mathcal{K}_0$. Recall (4) that

$$\bar{v}_{i\ell}^k = \begin{cases} \frac{\sum_{j \in N_i^k} v_{j\ell}^k}{\lambda_{i,\ell}^k}, & \text{if } \lambda_{i,\ell}^k \neq 0, \\ \mathbf{w}_{i\ell}^k, & \text{if } \lambda_{i,\ell}^k = 0. \end{cases} \tag{33}$$

Let ϖ^k be defined in (25), and ϖ_ℓ^k be its ℓ th entry. By (5), it follows

$$N_{i,\ell}^k := \{j \in N_i^k : v_{j\ell}^k \neq 0\}, \quad |N_{i,\ell}^k| = \lambda_{i,\ell}^k, \quad \varpi_\ell^k = \frac{1}{m} \sum_{i=1}^m w_{i\ell}^k, \quad \forall \ell \in [n]. \quad (34)$$

Moreover, if $\lambda_{i,\ell}^k = r > 0$ then

$$\bar{v}_{i\ell}^k = \frac{\sum_{j \in N_i^k} v_{j\ell}^k}{\lambda_{i,\ell}^k} = \frac{\sum_{j \in N_i^k} w_{j\ell}^k}{r} = \frac{\sum_{j \in N_{i,\ell}^k} w_{j\ell}^k}{r}. \quad (35)$$

Using the above facts, for any $\ell \in [n]$ and any $1 \leq r \leq t_i = |N_i^k|$, we have

$$\begin{aligned} \mathbb{E} (w_{i\ell}^k - \bar{v}_{i\ell}^k)^2 &= \sum_{r=1}^{t_i} \mathbb{P}(\lambda_{i,\ell}^k = r) \mathbb{E} \left[(w_{i\ell}^k - \bar{v}_{i\ell}^k)^2 \middle| \lambda_{i,\ell}^k = r \right] + \mathbb{P}(\lambda_{i,\ell}^k = 0) \mathbb{E} \left[(w_{i\ell}^k - \bar{v}_{i\ell}^k)^2 \middle| \lambda_{i,\ell}^k = 0 \right] \\ &\stackrel{(33,35)}{=} \sum_{r=1}^{t_i} \mathbb{P}(\lambda_{i,\ell}^k = r) \mathbb{E} \left[\left(w_{i\ell}^k - \frac{1}{r} \sum_{j \in N_{i,\ell}^k} w_{j\ell}^k \right)^2 \middle| \lambda_{i,\ell}^k = r \right] + \mathbb{P}(\lambda_{i,\ell}^k = 0) \mathbb{E} \left[(w_{i\ell}^k - w_{i\ell}^k)^2 \middle| \lambda_{i,\ell}^k = 0 \right] \\ &= \sum_{r=1}^{t_i} \mathbb{P}(\lambda_{i,\ell}^k = r) \mathbb{E} \left[\left(w_{i\ell}^k - \varpi_\ell^k - \frac{1}{r} \sum_{j \in N_{i,\ell}^k} (w_{j\ell}^k - \varpi_\ell^k) \right)^2 \middle| \lambda_{i,\ell}^k = r \right] \\ &\stackrel{(29)}{\leq} \sum_{r=1}^{t_i} \mathbb{P}(\lambda_{i,\ell}^k = r) \left(2(w_{i\ell}^k - \varpi_\ell^k)^2 + 2\mathbb{E} \left[\left(\frac{1}{r} \sum_{j \in N_{i,\ell}^k} (w_{j\ell}^k - \varpi_\ell^k) \right)^2 \middle| \lambda_{i,\ell}^k = r \right] \right) \\ &\stackrel{(30)}{\leq} 2(w_{i\ell}^k - \varpi_\ell^k)^2 \sum_{r=1}^{t_i} \mathbb{P}(\lambda_{i,\ell}^k = r) + \frac{2}{t_i} \sum_{j \in N_i^k} (w_{j\ell}^k - \varpi_\ell^k)^2 \sum_{r=1}^{t_i} \mathbb{P}(\lambda_{i,\ell}^k = r) \\ &\leq 2(w_{i\ell}^k - \varpi_\ell^k)^2 + \frac{2}{t_i} \sum_{j \in N_i^k} (w_{j\ell}^k - \varpi_\ell^k)^2. \end{aligned} \quad (36)$$

Additionally, we have

$$\begin{aligned} \sum_{i=1}^m \sum_{j \in N_i^k} \|\mathbf{w}_j^k - \varpi^k\|^2 &= \sum_{i=1}^m \sum_{j=1}^m \mathbb{I}(j \in N_i^k) \|\mathbf{w}_j^k - \varpi^k\|^2 \\ &= \sum_{j=1}^m \|\mathbf{w}_j^k - \varpi^k\|^2 \sum_{i=1}^m \mathbb{I}(j \in N_i^k) \\ &\leq m \sum_{i=1}^m \|\mathbf{w}_i^k - \varpi^k\|^2. \end{aligned} \quad (37)$$

where $\mathbb{I}(j \in N)$ is an indicator function defined by (19). Combine the above facts yields

$$\begin{aligned} \sum_{i=1}^m 2t_i \mathbb{E} \|\mathbf{w}_i^k - \bar{\mathbf{v}}_i^k\|^2 &= 2 \sum_{i=1}^m t_i \sum_{\ell=1}^n \mathbb{E} [(w_{i\ell}^k - v_{i\ell}^k)^2] \\ &\stackrel{(36)}{\leq} 2 \sum_{i=1}^m t_i \sum_{\ell=1}^n \left(2(w_{i\ell}^k - \varpi_\ell^k)^2 + \frac{2}{t_i} \sum_{j \in N_i^k} (w_{j\ell}^k - \varpi_\ell^k)^2 \right) \\ &= 4 \sum_{i=1}^m t_i \|\mathbf{w}_i^k - \varpi^k\|^2 + 4 \sum_{i=1}^m \sum_{j \in N_i^k} \|\mathbf{w}_j^k - \varpi^k\|^2 \\ &\stackrel{(37)}{\leq} 8m \|\mathbf{W}^k - \mathbf{\Pi}^k\|_F^2. \end{aligned} \quad (38)$$

where the last inequality uses $t_i = |N_i^k| \leq |N_i| = m_i \leq m$. The second condition in (32) follows $t_i \geq t_{\min}$ \square

Lemma 3. Let $\{(\mathbf{W}^k, \mathbf{V}^k)\}$ be the sequence generated by Algorithm 1 with Setup 1. Then under Assumptions 1 and 2,

$$\mathbf{w}_i^k \in \mathbb{N}(2\delta), \quad \bar{\mathbf{v}}_i^k \in \mathbb{N}(2\delta), \quad \forall i \in [m], k \geq 0.$$

Proof. We first claim that for any $k \geq 0$,

$$\|\mathbf{w}_i^k\|_\infty \leq \phi, \quad \forall i \in [m] \implies \|\bar{\mathbf{v}}_i^k\|_\infty \leq \phi, \quad \forall i \in [m]. \quad (39)$$

In fact, when $k \notin \mathcal{K}_0$,

$$\|\bar{\mathbf{v}}_i^k\|_\infty = \|\mathbf{w}_i^k\|_\infty \leq \phi.$$

When $k \in \mathcal{K}_0$, we consider two cases:

- If $\lambda_{i,\ell}^k = 0$, we have

$$|\bar{v}_{i\ell}^k| \stackrel{(4)}{=} |w_{i\ell}^k| \leq \phi.$$

- If $\lambda_{i,\ell}^k \neq 0$,

$$|\bar{v}_{i\ell}^k| \stackrel{(4)}{\leq} \frac{\sum_{j \in N_i^k} |v_{j\ell}^k|}{\lambda_{i,\ell}^k} \stackrel{(35)}{=} \frac{\sum_{j \in N_{i,\ell}^k} |w_{j\ell}^k|}{|N_{i,\ell}^k|} \leq \frac{\sum_{j \in N_{i,\ell}^k} \phi}{|N_{i,\ell}^k|} = \phi.$$

Both cases yield $\|\bar{\mathbf{v}}_i^k\|_\infty \leq \phi$, showing (39). Recall (16) that

$$\sigma^0 \geq \sigma \geq \frac{\varepsilon(2\delta)\gamma}{(\gamma-1)\delta t_{\min}}.$$

This condition indicates

$$\sum_{j=0}^k \frac{\varepsilon_i(2\delta)}{\sigma^j t_i} \leq \sum_{j=0}^{\infty} \frac{\varepsilon_i(2\delta)}{\sigma^j t_i} = \frac{\varepsilon_i(2\delta)}{\sigma^0 t_i} \sum_{j=0}^{\infty} \frac{1}{\gamma^j} \leq \frac{\varepsilon_i(2\delta)}{\sigma^0 t_i} \frac{\gamma}{\gamma-1} \stackrel{(14)}{\leq} \frac{\varepsilon(2\delta)}{\sigma t_{\min}} \frac{\gamma}{\gamma-1} \leq \delta. \quad (40)$$

- When $j = 0$, the algorithm has initializations $\mathbf{w}_i^0 = 0$ for all $i \in [m]$, namely, for any $i \in [m]$,

$$\|\mathbf{w}_i^0\|_\infty \leq \delta \leq 2\delta, \quad \|\bar{\mathbf{v}}_i^0\|_\infty \stackrel{(39)}{\leq} \delta \leq 2\delta. \quad (41)$$

- When $j = 1$, according to (21), for any $i \in [m]$,

$$\begin{aligned} \|\mathbf{w}_i^1\|_\infty &\stackrel{(21)}{\leq} \|\bar{\mathbf{v}}_i^0\|_\infty + \|\mathbf{h}_i^0\|_\infty \\ &\stackrel{(41)}{\leq} \delta + \|\mathbf{h}_i^0\|_\infty \\ &\stackrel{(22)}{=} \delta + \frac{1}{\sigma^0 t_i} \|\mathbf{g}_i^0\|_\infty \\ &\stackrel{(14,41)}{\leq} \delta + \frac{\varepsilon_i(2\delta)}{\sigma^0 t_i} \stackrel{(40)}{\leq} 2\delta, \\ \|\bar{\mathbf{v}}_i^1\|_\infty &\stackrel{(39)}{\leq} \delta + \frac{\varepsilon_i(2\delta)}{\sigma^0 t_i} \leq 2\delta. \end{aligned} \quad (42)$$

- When $j = 2$, using the similar reasoning to show (42) enables the following conditions,

$$\begin{aligned} \|\mathbf{w}_i^2\|_\infty &\leq \delta + \frac{\varepsilon_i(2\delta)}{\sigma^0 t_i} + \frac{\varepsilon_i(2\delta)}{\sigma^1 t_i} \stackrel{(40)}{\leq} 2\delta, \\ \|\bar{\mathbf{v}}_i^2\|_\infty &\stackrel{(39)}{\leq} \delta + \frac{\varepsilon_i(2\delta)}{\sigma^0 t_i} + \frac{\varepsilon_i(2\delta)}{\sigma^1 t_i} \leq 2\delta. \end{aligned} \quad (43)$$

- When $j = k$, using the similar reasoning to show (43) enables the following conditions,

$$\begin{aligned} \|\mathbf{w}_i^k\|_\infty &\leq \delta + \sum_{j=0}^{k-1} \frac{\varepsilon_i(2\delta)}{\sigma^j t_i} \stackrel{(40)}{\leq} 2\delta, \\ \|\bar{\mathbf{v}}_i^k\|_\infty &\stackrel{(39)}{\leq} \delta + \sum_{j=0}^{k-1} \frac{\varepsilon_i(2\delta)}{\sigma^j t_i} \leq 2\delta. \end{aligned}$$

This shows the desired result. \square

Lemma 4. Let $\{(\mathbf{W}^k, \mathbf{V}^k)\}$ be the sequence generated by Algorithm 1 with Setup 1. For every $i \in [m]$, let

$$\begin{aligned} \varrho_i &:= (1-p)^{t_i}, \\ c_i &:= \sum_{r=1}^{t_i} \binom{t_i}{r} p^r (1-p)^{t_i-r} \frac{t_i-r}{r(t_i-1)}, \\ \xi_i &:= \frac{(1-\varrho_i)(m_i-t_i)}{m_i t_i (m_i-1)}, \\ C_1 &:= \max_i \left\{ \varrho_i (1+\zeta)^2 + \sum_{j \in N_i} \left(\frac{c_j}{m_j} + \xi_j \right) \right\}. \end{aligned} \quad (44)$$

Here, we denote $0/0 = 0$ and thus $c_i = 0$ when $t_i = 1$. Then

$$\zeta + \sqrt{C_1} < \frac{1}{\gamma^{k_0/2}}. \quad (45)$$

Proof. For $t_i = 1$, $c_i = 0 \leq 1 - (1-p) = 1 - \varrho_i$. For $t_i \geq 2$,

$$c_i \leq \sum_{r=1}^{t_i} \binom{t_i}{r} p^r (1-p)^{t_i-r} = 1 - (1-p)^{t_i} = 1 - \varrho_i.$$

Using this fact and the definition of ξ_j , we obtain

$$\frac{c_j}{m_j} + \xi_j \leq \frac{(1-\varrho_j)(t_j m_j + m_j - 2t_j)}{t_j m_j (m_j - 1)}.$$

By Bernoulli's inequality, $1 - \varrho_j = 1 - (1-p)^{t_j} \leq t_j p$. Using this condition and $t_j = \lfloor \nu_j m_j \rfloor$ yields

$$\begin{aligned} \sum_{j \in N_i} \left(\frac{\nu_j}{m_j} + \xi_j \right) &\leq p \sum_{j \in N_i} \frac{t_j m_j + m_j - 2t_j}{m_j (m_j - 1)} \\ &\leq p \sum_{j \in N_i} \frac{\lfloor \nu_j m_j \rfloor (m_j - 2) + m_j}{m_j (m_j - 1)} \\ &\leq p \sum_{j \in N_i} \frac{\nu_j (m_j - 2) + 1}{m_j - 1} \\ &\leq 2p \sum_{j \in N_i} \nu_j, \end{aligned}$$

which results in

$$\varrho_i (1+\zeta)^2 + \sum_{j \in N_i} \left(\frac{c_j}{m_j} + \xi_j \right) \leq \varrho_i (1+\zeta)^2 + 2p \sum_{j \in N_i} \nu_j \stackrel{(11)}{<} \left(\frac{1}{\gamma^{k_0/2}} - \zeta \right)^2,$$

for any $i \in [m]$, and hence $\sqrt{C_1} < \gamma^{-k_0/2} - \zeta$, showing the desired result. \square

Lemma 5. Let $\{(\mathbf{W}^k, \mathbf{V}^k)\}$ be the sequence generated by Algorithm 1 with Setup 1 and C_1 be defined by (44). Then under Assumptions 1 and 2, it holds

$$\mathbb{E} \|\mathbf{P}^k\|_F^2 \leq C_1 \mathbb{E} \|\mathbf{W}^k - \mathbf{\Pi}^k\|_F^2, \quad \forall k \in \mathcal{K}_0. \quad (46)$$

Proof. Let $\widehat{\mathbf{w}}_i^k$ and $\widetilde{\mathbf{w}}_i^k$ be defined by (25) and $\widehat{w}_{i\ell}^k$ and $\widetilde{w}_{i\ell}^k$ be their ℓ th entry. Following the notation in Lemma 2, let $N_{i,\ell}^k \subseteq N_i^k$ be defined in (34) and $\lambda_{i,\ell}^k = |N_{i,\ell}^k|$. To bound

$$\mathbf{P}^k = \mathbf{V}^k - \mathbf{W}^k \mathbf{B} = (\overline{\mathbf{v}}_1^k - \widehat{\mathbf{w}}_1^k, \overline{\mathbf{v}}_2^k - \widehat{\mathbf{w}}_2^k, \dots, \overline{\mathbf{v}}_m^k - \widehat{\mathbf{w}}_m^k),$$

as shown in (26), it suffices to bound $\|\bar{\mathbf{v}}_i^k - \hat{\mathbf{w}}_i^k\|$ or $\bar{v}_{i\ell}^k - \hat{w}_{i\ell}^k$. Therefore, condition on the random neighbor set N_i^k , for any $1 \leq r \leq t_i = |N_i^k|$, we have

$$\begin{aligned}
 \mathbb{E} \left[\left(\bar{v}_{i\ell}^k - \hat{w}_{i\ell}^k \right)^2 \mid \lambda_{i,\ell}^k = r \right] &\stackrel{(35)}{=} \mathbb{E} \left[\left(\frac{1}{r} \sum_{j \in N_{i,\ell}^k} w_{j\ell}^k - \hat{w}_{i\ell}^k + \tilde{w}_{i\ell}^k - \hat{w}_{i\ell}^k \right)^2 \mid \lambda_{i,\ell}^k = r \right] \\
 &= \mathbb{E} \left[\left(\frac{1}{r} \sum_{j \in N_{i,\ell}^k} w_{j\ell}^k - \hat{w}_{i\ell}^k \right)^2 \mid \lambda_{i,\ell}^k = r \right] + \mathbb{E} \left[\left(\tilde{w}_{i\ell}^k - \hat{w}_{i\ell}^k \right)^2 \mid \lambda_{i,\ell}^k = r \right] \\
 &\stackrel{(31)}{=} \frac{t_i - r}{rt_i(t_i - 1)} \sum_{j \in N_i^k} (w_{j\ell}^k - \tilde{w}_{i\ell}^k)^2 + (\tilde{w}_{i\ell}^k - \hat{w}_{i\ell}^k)^2,
 \end{aligned} \tag{47}$$

where the second equation used the following fact,

$$\begin{aligned}
 &\mathbb{E} \left[2 \left(\frac{1}{r} \sum_{j \in N_{i,\ell}^k} w_{j\ell}^k - \hat{w}_{i\ell}^k \right) (\tilde{w}_{i\ell}^k - \hat{w}_{i\ell}^k) \mid \lambda_{i,\ell}^k = r \right] \\
 &= \mathbb{E} \left[2 \left(\frac{1}{r} \sum_{j \in N_{i,\ell}^k} w_{j\ell}^k - \hat{w}_{i\ell}^k \right) \mid \lambda_{i,\ell}^k = r \right] (\tilde{w}_{i\ell}^k - \hat{w}_{i\ell}^k) \\
 &= 2 \left(\mathbb{E} \left[\frac{1}{r} \sum_{j \in N_{i,\ell}^k} w_{j\ell}^k \mid \lambda_{i,\ell}^k = r \right] - \hat{w}_{i\ell}^k \right) (\tilde{w}_{i\ell}^k - \hat{w}_{i\ell}^k) \\
 &= 2 \left(\frac{1}{t_i} \sum_{j \in N_i^k} w_{j\ell}^k - \hat{w}_{i\ell}^k \right) (\tilde{w}_{i\ell}^k - \hat{w}_{i\ell}^k) = 0.
 \end{aligned}$$

We point out that if $t_i = 1$, then

$$\sum_{j \in N_i^k} (w_{j\ell}^k - \hat{w}_{i\ell}^k)^2 = (w_{j\ell}^k - w_{j\ell}^k)^2 = 0, \tag{48}$$

which means (47) still holds. In this scenario, we let $0/0 = 0$. According to Setup 1, each node $j \in N_i^k$ independently constructs a set $T_j^k \subseteq [n]$ by uniformly selecting s entries of $[n]$ without replacement. This indicates that each entry of \mathbf{w}_j^k will be selected in a probability $p = s/n$. Consequently,

$$\mathbb{P}(\lambda_{i,\ell}^k = 0) = (1-p)^{t_i} = \varrho_i, \quad \mathbb{P}(\lambda_{i,\ell}^k = r) = \binom{t_i}{r} p^r (1-p)^{t_i-r}, \quad \sum_{r=1}^{t_i} \mathbb{P}(\lambda_{i,\ell}^k = r) = 1 - \varrho_i. \tag{49}$$

where ϱ_i is defined by (44). Using these fact enable us to derive that

$$\begin{aligned}
 &\mathbb{E} \left[(\bar{v}_{i\ell}^k - \hat{w}_{i\ell}^k)^2 \mid \lambda_{i,\ell}^k = r \right] \\
 &= \mathbb{P}(\lambda_{i,\ell}^k = 0) \mathbb{E} \left[(\bar{v}_{i\ell}^k - \hat{w}_{i\ell}^k)^2 \mid \lambda_{i,\ell}^k = 0 \right] + \sum_{r=1}^{t_i} \mathbb{P}(\lambda_{i,\ell}^k = r) \mathbb{E} \left[(\bar{v}_{i\ell}^k - \hat{w}_{i\ell}^k)^2 \mid \lambda_{i,\ell}^k = r \right] \\
 &\stackrel{(33)}{=} \mathbb{P}(\lambda_{i,\ell}^k = 0) \mathbb{E} \left[(w_{i\ell}^k - \hat{w}_{i\ell}^k)^2 \mid \lambda_{i,\ell}^k = 0 \right] + \sum_{r=1}^{t_i} \mathbb{P}(\lambda_{i,\ell}^k = r) \mathbb{E} \left[(\bar{v}_{i\ell}^k - \hat{w}_{i\ell}^k)^2 \mid \lambda_{i,\ell}^k = r \right] \\
 &\stackrel{(47)}{=} \mathbb{P}(\lambda_{i,\ell}^k = 0) (w_{i\ell}^k - \hat{w}_{i\ell}^k)^2 + \sum_{r=1}^{t_i} \mathbb{P}(\lambda_{i,\ell}^k = r) \left(\frac{t_i - r}{r(t_i - 1)} \frac{1}{t_i} \sum_{j \in N_i^k} (w_{j\ell}^k - \tilde{w}_{i\ell}^k)^2 + (\tilde{w}_{i\ell}^k - \hat{w}_{i\ell}^k)^2 \right) \\
 &\stackrel{(49)}{=} \varrho_i (w_{i\ell}^k - \hat{w}_{i\ell}^k)^2 + \frac{c_i}{t_i} \sum_{j \in N_i^k} (w_{j\ell}^k - \tilde{w}_{i\ell}^k)^2 + (1 - \varrho_i) (\tilde{w}_{i\ell}^k - \hat{w}_{i\ell}^k)^2,
 \end{aligned} \tag{50}$$

where c_i is defined by (44). Here we let $c_i = 0$ due to (48). Now we bound the three terms in (50) separately.

- For the first term, by $\mathbf{W}^k \mathbf{B} = (\hat{\mathbf{w}}_1^k, \dots, \hat{\mathbf{w}}_m^k)$, we have

$$\sum_{i=1}^m \|\mathbf{w}_i^k - \hat{\mathbf{w}}_i^k\|^2 = \|\mathbf{W}^k (\mathbf{I} - \mathbf{B})\|_F^2 \stackrel{(27)}{=} \|\mathbf{W}^k (\mathbf{I} - \mathbf{B}) - \mathbf{\Pi}^k (\mathbf{I} - \mathbf{B})\|_F^2 \stackrel{(9)}{\leq} (1 + \zeta)^2 \|\mathbf{W}^k - \mathbf{\Pi}^k\|_F^2. \tag{51}$$

- For the second term, taking expectation with respect to N_i^k gives

$$\begin{aligned}
 \mathbb{E} \left[\sum_{i=1}^m \frac{c_i}{t_i} \sum_{j \in N_i^k} \|\mathbf{w}_j^k - \tilde{\mathbf{w}}_i^k\|^2 \right] &\leq \mathbb{E} \left[\sum_{i=1}^m \frac{c_i}{t_i} \sum_{j \in N_i^k} \|\mathbf{w}_j^k - \boldsymbol{\varpi}^k\|^2 \right] \\
 &= \sum_{i=1}^m \frac{c_i}{m_i} \sum_{j \in N_i} \|\mathbf{w}_j^k - \boldsymbol{\varpi}^k\|^2 \\
 &= \sum_{i=1}^m \sum_{j \in N_i} \frac{\nu_j}{m_j} \|\mathbf{w}_i^k - \boldsymbol{\varpi}^k\|^2,
 \end{aligned} \tag{52}$$

where the first inequality is from (25), that is, $\boldsymbol{\varpi}^k$ and $\tilde{\mathbf{w}}_i^k$ are the mean of $\{\mathbf{w}_j^k : j \in [m]\}$ and $\{\mathbf{w}_j^k : j \in N_i^k\}$ and the last equality is derived by exchanging the summation indices i and j using the undirected-graph property.

- For the third term, we apply the variance formula for simple random sampling with respect to N_i^k ,

$$\begin{aligned}
 \sum_{i=1}^m (1 - \varrho_i) \mathbb{E} \|\tilde{\mathbf{w}}_i^k - \hat{\mathbf{w}}_i^k\|^2 &\stackrel{(31)}{=} \sum_{i=1}^m \frac{1 - \varrho_i}{m_i} \frac{m_i - t_i}{t_i(m_i - 1)} \sum_{j \in N_i} \|\mathbf{w}_j^k - \hat{\mathbf{w}}_i^k\|^2 \\
 &\stackrel{(44)}{=} \sum_{i=1}^m \xi_j \sum_{j \in N_i} \|\mathbf{w}_j^k - \hat{\mathbf{w}}_i^k\|^2 \\
 &\leq \sum_{i=1}^m \sum_{j \in N_i} \xi_j \|\mathbf{w}_i^k - \boldsymbol{\varpi}^k\|^2,
 \end{aligned} \tag{53}$$

where the first inequality is from (25), that is, $\boldsymbol{\varpi}^k$ and $\hat{\mathbf{w}}_i^k$ are the mean of $\{\mathbf{w}_j^k : j \in [m]\}$ and $\{\mathbf{w}_j^k : j \in N_i\}$. Finally, combining (50) with (51)–(53) and applying the law of total expectation, we obtain

$$\mathbb{E} \|\mathbf{P}^k\|_F^2 = \sum_{i=1}^m \mathbb{E} \|\bar{\mathbf{v}}_i^k - \hat{\mathbf{w}}_i^k\|^2 \leq C_1 \|\mathbf{W}^k - \boldsymbol{\Pi}^k\|_F^2. \tag{54}$$

where C_1 is defined by (44). Therefore, we arrive at (46). Here, the expectation in (54) is taken over the randomness at round k (conditioned on \mathbf{W}^k), while (46) further averages over all randomness accumulated up to round k . \square

Lemma 6. *Let $\{(\mathbf{W}^k, \mathbf{V}^k)\}$ be the sequence generated by Algorithm 1 with Setup 1. Then under Assumptions 1 and 2, there exist constants $C_2 > 0$ and $\beta > \gamma$ such that*

$$\mathbb{E} \left\| \mathbf{W}^k - \boldsymbol{\Pi}^k \right\|_F^2 \leq \frac{C_2}{\beta^k}. \tag{55}$$

Proof. For compactness, we define the expected consensus error and the gradient heterogeneity term at step k as

$$\mathcal{W}^k := \mathbb{E} \left\| \mathbf{W}^k - \boldsymbol{\Pi}^k \right\|_F^2, \quad \mathcal{G}^k := \mathbb{E} \|\mathbf{H}^k(\mathbf{I} - \mathbf{J})\|_F^2. \tag{56}$$

By Lemma 3, we have $\bar{\mathbf{v}}_i^k \in \mathbb{N}(2\delta)$ and thus

$$\|\mathbf{g}_i^k\|^2 \stackrel{(22)}{=} \|\nabla f(\bar{\mathbf{v}}_i^k; \mathcal{B}_i^k)\|^2 \leq n \|\nabla f(\bar{\mathbf{v}}_i^k; \mathcal{B}_i^k)\|_\infty^2 \stackrel{(12)}{\leq} n \varepsilon_i^2(2\delta) \stackrel{(14)}{\leq} n \varepsilon^2(2\delta). \tag{57}$$

As $t_{\min} = \min\{t_1, t_2, \dots, t_m\}$, $\sigma^k = \sigma^0 \gamma^k \geq \sigma \gamma^k$, and $\|\mathbf{I} - \mathbf{J}\| = 1$, we have

$$\begin{aligned}
 \mathcal{G}^k &\stackrel{(56)}{\leq} \mathbb{E} \|\mathbf{H}^k\|_F^2 \stackrel{(24)}{=} \mathbb{E} \|\mathbf{G}^k \mathbf{D}^k\|_F^2 \leq \mathbb{E} \|\mathbf{D}^k\|^2 \|\mathbf{G}^k\|_F^2 \\
 &\stackrel{(23)}{=} \frac{\mathbb{E} \|\mathbf{G}^k\|_F^2}{\sigma^{2k} t_{\min}^2} \leq \frac{1}{\sigma^{2k} t_{\min}^2} \sum_{i=1}^m \mathbb{E} \|\mathbf{g}_i^k\|^2 \leq \frac{\Gamma}{\gamma^{2k}}, \quad \text{with } \Gamma := \frac{mn \varepsilon^2(2\delta)}{\sigma^2 t_{\min}^2}.
 \end{aligned} \tag{58}$$

Let $\iota > 0$ satisfy

$$\iota \in \left(0, \frac{1}{\gamma (\zeta + \sqrt{C_1})^{2/k_0}} - 1 \right). \tag{59}$$

The above range is well defined due to (45). Then define

$$\rho_1 := 1 + \iota, \quad \rho_2 := 1 + \frac{1}{\iota}, \quad \rho := \rho_1 (\zeta + \sqrt{C_1})^2. \tag{60}$$

It is easy to check that

$$\rho \rho_1^{k_0-1} = (1 + \iota)^{k_0} (\zeta + \sqrt{C_1})^2 \stackrel{(59)}{<} \frac{1}{\gamma^{k_0}}. \tag{61}$$

Case 1: $k \notin \mathcal{K}_0$. Algorithm 1 states that $\bar{\mathbf{v}}_i^k = \mathbf{w}_i^k$. Recalling the update rule (28) and, the consensus error evolves as

$$\mathbf{W}^{k+1} - \mathbf{\Pi}^{k+1} \stackrel{(26)}{=} \mathbf{W}^k - \mathbf{H}^k - (\mathbf{W}^k - \mathbf{H}^k)\mathbf{J} = (\mathbf{W}^k - \mathbf{\Pi}^k) - \mathbf{H}^k(\mathbf{I} - \mathbf{J}). \quad (62)$$

Taking the Frobenius norm, taking expectation, and using Young's inequality with constant ι , we obtain

$$\mathcal{W}^{k+1} \stackrel{(29)}{\leq} \rho_1 \mathcal{W}^k + \rho_2 \mathcal{G}^k \stackrel{(58)}{\leq} \rho_1 \mathcal{W}^k + \frac{\rho_2 \Gamma}{\gamma^{2k}}. \quad (63)$$

Case 2: $k \in \mathcal{K}_0$. By the definition of $\mathbf{P}^k = \mathbf{V}^k - \mathbf{W}^k \mathbf{B}$ and $\mathbf{J} \mathbf{B} = \mathbf{B} \mathbf{J} = \mathbf{J}$ from (8),

$$\begin{aligned} \mathbf{W}^{k+1} - \mathbf{\Pi}^{k+1} &\stackrel{(27)}{=} \mathbf{W}^{k+1}(\mathbf{I} - \mathbf{J}) \\ &\stackrel{(28)}{=} (\mathbf{W}^k \mathbf{B} - \mathbf{H}^k + \mathbf{P}^k)(\mathbf{I} - \mathbf{J}) \\ &\stackrel{(27)}{=} \mathbf{W}^k(\mathbf{B} - \mathbf{J}) - \mathbf{\Pi}^k(\mathbf{B} - \mathbf{J}) + \mathbf{P}^k(\mathbf{I} - \mathbf{J}) - \mathbf{H}^k(\mathbf{I} - \mathbf{J}) \\ &= (\mathbf{W}^k - \mathbf{\Pi}^k)(\mathbf{B} - \mathbf{J}) + \mathbf{P}^k(\mathbf{I} - \mathbf{J}) - \mathbf{H}^k(\mathbf{I} - \mathbf{J}). \end{aligned} \quad (64)$$

Applying Young's inequality twice with constants $\iota > 0$, we have

$$\begin{aligned} \mathcal{W}^{k+1} &\leq \rho_1 \mathbb{E} \left\| (\mathbf{W}^k - \mathbf{\Pi}^k)(\mathbf{B} - \mathbf{J}) + \mathbf{P}^k(\mathbf{I} - \mathbf{J}) \right\|_F^2 + \rho_2 \mathcal{G}^k \\ &\leq \rho_1 \left[\left(1 + \frac{\sqrt{C_1}}{\zeta}\right) \mathbb{E} \|\mathbf{W}^k - \mathbf{\Pi}^k\|_F^2 + \left(1 + \frac{\zeta}{\sqrt{C_1}}\right) \mathbb{E} \|\mathbf{P}^k\|_F^2 \right] + \rho_2 \mathcal{G}^k \\ &\stackrel{(9)}{\leq} \rho_1 \left[(\zeta^2 + \zeta \sqrt{C_1}) \mathcal{W}^k + \left(1 + \frac{\zeta}{\sqrt{C_1}}\right) \mathbb{E} \|\mathbf{P}^k\|_F^2 \right] + \rho_2 \mathcal{G}^k \\ &\stackrel{(46)}{\leq} \rho_1 (\zeta^2 + \zeta \sqrt{C_1} + C_1 + \zeta \sqrt{C_1}) \mathcal{W}^k + \rho_2 \mathcal{G}^k \\ &\stackrel{(60,58)}{\leq} \rho \mathcal{W}^k + \frac{\rho_2 \Gamma}{\gamma^{2k}}, \end{aligned} \quad (65)$$

where the second inequality also used $\|\mathbf{I} - \mathbf{J}\|_2 = 1$. At the communication step $k = ak_0$, according to (65),

$$\mathcal{W}^{ak_0+1} \leq \rho \mathcal{W}^{ak_0} + \frac{\rho_2 \Gamma}{\gamma^{2ak_0}} \quad (66)$$

Denote

$$M := (\rho \rho_1^{k_0-1})^{1/k_0} \stackrel{(61)}{<} \frac{1}{\gamma}, \quad P := P(k_0), \quad \text{with } P(t) := \rho_2 \Gamma \left(\rho_1^{t-1} + \sum_{j=1}^{t-1} \frac{\rho_1^{t-1-j}}{\gamma^{2j}} \right). \quad (67)$$

One can verify that

$$P \leq \frac{\rho_2 \rho_1^{k_0} \gamma^2 \Gamma}{\rho_1 \gamma^2 - 1}.$$

For any $2 \leq t \leq k_0$, applying (63) recursively yields,

$$\begin{aligned} \mathcal{W}^{ak_0+t} &\leq \rho_1^{t-1} \mathcal{W}^{ak_0+1} + \rho_2 \Gamma^2 \sum_{j=1}^{t-1} \frac{\rho_1^{t-1-j}}{\gamma^{2(ak_0+j)}} \\ &\stackrel{(66)}{\leq} \rho \rho_1^{t-1} \mathcal{W}^{ak_0} + \frac{P(t)}{\gamma^{2ak_0}} \\ &\leq M^{k_0} \mathcal{W}^{ak_0} + \frac{P}{\gamma^{2ak_0}}. \end{aligned}$$

Since $\rho < M^{k_0}$ and $\rho_2 \Gamma \leq P$, by (66), the above inequality also holds for $t = 1$. Overall,

$$\mathcal{W}^{ak_0+t} \leq M^{k_0} \mathcal{W}^{ak_0} + \frac{P}{\gamma^{2ak_0}}, \quad \forall t = 1, 2, \dots, k_0. \quad (68)$$

In particular, when $t = k_0$,

$$\mathcal{W}^{(a+1)k_0} \leq M^{k_0} \mathcal{W}^{ak_0} + \frac{P}{\gamma^{2ak_0}}, \quad \forall a = 0, 1, 2, \dots. \quad (69)$$

According to the initialization of Algorithm 1, $\mathbf{W}^0 = 0$, we have $\mathcal{W}^0 = 0$. Iterating (69) yields, for any $a \geq 1$,

$$\mathcal{W}^{ak_0} \leq M^{ak_0} \mathcal{W}^0 + P \sum_{\tau=0}^{a-1} \frac{M^{(a-1-\tau)k_0}}{\gamma^{2\tau k_0}} = \frac{P(M^{ak_0} - \gamma^{-2ak_0})}{M - \gamma^{-2}}.$$

Note that M depends continuously on ι . Thus, we can always select an ι within the range defined in (59) to strictly ensure $M \neq \gamma^{-2}$ without violating (61). Therefore, the above condition leads to

$$\mathcal{W}^{ak_0} \leq Q\varphi^{ak_0}, \quad \text{with } \varphi := \max\{M, \gamma^{-2}\} \in (0, 1), \quad Q := \frac{P}{|M - \gamma^{-2}|}. \quad (70)$$

Now for any $t = 1, 2, \dots, k_0 - 1$,

$$\begin{aligned} \mathcal{W}^{ak_0+t} &\stackrel{(68)}{\leq} M^{k_0} \mathcal{W}^{ak_0} + \frac{P}{\gamma^{2ak_0}} \\ &\stackrel{(61)}{\leq} \frac{\mathcal{W}^{ak_0}}{\gamma} + \frac{P}{\gamma^{2ak_0}} \\ &\stackrel{(70)}{\leq} (Q + P)\varphi^{ak_0}. \end{aligned}$$

This together with (70) indicates that for any $t = 1, 2, \dots, k_0$,

$$\mathcal{W}^{ak_0+t} \leq (Q + P)\varphi^{ak_0} = \frac{Q + P}{\varphi^t} \varphi^{ak_0+t} \leq \frac{Q + P}{\varphi^{k_0}} \varphi^{ak_0+t}. \quad (71)$$

Now let

$$\beta := \frac{1}{\varphi} = \min\left\{\frac{1}{M}, \gamma^2\right\} = \min\left\{\frac{1}{(\rho\rho_1^{k_0-1})^{1/k_0}}, \gamma^2\right\} \stackrel{(61)}{>} \min\{\gamma, \gamma^2\} = \gamma,$$

which together with (71) leads to

$$\mathcal{W}^k \leq \frac{Q + P}{\varphi^{k_0}} \frac{1}{\beta^k},$$

showing the desired result. \square

C. Main Results

Recall that

$$H^k := H(\mathbf{W}^k, \mathbf{V}^k, \boldsymbol{\sigma}^k) := \mathbb{E} \sum_{i=1}^n \left(f_i(\mathbf{w}_i^k) + \frac{\sigma_i^k t_i}{2} \|\mathbf{w}_i^k - \bar{\mathbf{v}}_i^k\|^2 \right), \quad \tilde{H}^k := H^k + \frac{C}{\gamma^k} + \frac{D}{\eta^k}. \quad (72)$$

Here, the involved constants are defined as

$$\eta := \frac{\beta}{\gamma} > 1, \quad C := \frac{\gamma}{\gamma - 1} \frac{4mn\varepsilon^2(2\delta)}{\sigma t_{\min}}, \quad D = \frac{\eta}{\eta - 1} \frac{4(1 + \gamma)m\sigma^0 C_2}{\beta}, \quad (73)$$

where $\beta > \gamma$ and C_2 are defined in Lemma 6.

Lemma 7. *Let $\{(\mathbf{W}^k, \mathbf{V}^k)\}$ be the sequence generated by Algorithm 1 with Setup 1. Then under Assumptions 1 and 2,*

$$\tilde{H}^k \geq H^k > -\infty. \quad (74)$$

Proof. From Lemma 3, we have $\mathbf{w}_i^k \in \mathbb{N}(2\delta)$, which contribute to

$$\begin{aligned} f_i(\bar{\mathbf{v}}_i^k) &\stackrel{(17)}{\leq} f_i(\mathbf{w}_i^k) + \langle \nabla f_i(\mathbf{w}_i^k), \bar{\mathbf{v}}_i^k - \mathbf{w}_i^k \rangle + \frac{\sigma_i^k}{8} \|\mathbf{w}_i^k - \bar{\mathbf{v}}_i^k\|^2 \\ &\stackrel{(29)}{\leq} f_i(\mathbf{w}_i^k) + \frac{2}{\sigma_i^k t_{\min}} \|\nabla f_i(\mathbf{w}_i^k)\|^2 + \frac{(t_{\min} + 1)\sigma_i^k}{8} \|\mathbf{w}_i^k - \bar{\mathbf{v}}_i^k\|^2 \\ &\leq f_i(\mathbf{w}_i^k) + \frac{2n}{\sigma_i^k t_{\min}} \|\nabla f_i(\mathbf{w}_i^k)\|_\infty^2 + \frac{\sigma_i^k t_{\min}}{4} \|\mathbf{w}_i^k - \bar{\mathbf{v}}_i^k\|^2 \\ &\stackrel{(12)}{\leq} f_i(\mathbf{w}_i^k) + \frac{2n\varepsilon^2(2\delta)}{\sigma_i^k t_{\min}} + \frac{\sigma_i^k t_{\min}}{4} \|\mathbf{w}_i^k - \bar{\mathbf{v}}_i^k\|^2, \end{aligned}$$

where the last two inequalities are from $t_{\min} \geq 1$ and $\varepsilon_i(2\delta) \leq \varepsilon(2\delta)$. Therefore, we obtain

$$\begin{aligned}
 \tilde{H}^k \geq H^k &\geq \mathbb{E} \sum_{i=1}^m \left(f_i(\mathbf{w}_i^k) + \frac{\sigma^k t_{\min}}{2} \|\mathbf{w}_i^k - \bar{\mathbf{v}}_i^k\|^2 \right) \\
 &\stackrel{\text{(III-C)}}{\geq} \mathbb{E} \sum_{i=1}^m \left(f_i(\bar{\mathbf{v}}_i^k) - \frac{2n\varepsilon^2(2\delta)}{\sigma^k t_{\min}} + \frac{\sigma^k t_{\min}}{4} \|\mathbf{w}_i^k - \bar{\mathbf{v}}_i^k\|^2 \right) \\
 &\stackrel{\text{(18)}}{\geq} f^* - \frac{2mn\varepsilon^2(2\delta)}{\sigma^k t_{\min}} \\
 &\stackrel{\text{(16)}}{\geq} f^* - \frac{2mn\varepsilon^2(2\delta)}{\sigma t_{\min}} > -\infty.
 \end{aligned}$$

This completes the proof. \square

D. Proof of Theorem 2.

Theorem 2. Let $\{(\mathbf{W}^k, \mathbf{V}^k)\}$ be the sequence generated by Algorithm 1 with Setup 1. Then the following statements hold under Assumptions 1 and 2.

- 1) For any $k \geq 0$ and $i \in [m]$, $\mathbf{w}_i^k \in \mathbb{N}(2\delta)$ and $\bar{\mathbf{v}}_i^k \in \mathbb{N}(2\delta)$.
- 2) For any $k \geq 0$,

$$\tilde{H}^k - \tilde{H}^{k+1} \geq \sum_{i=1}^m \frac{\sigma_i^k t_i}{8} \left(\|\Delta \mathbf{w}_i^{k+1}\|^2 + \|\Delta \bar{\mathbf{v}}_i^{k+1}\|^2 \right), \quad (75)$$

where \tilde{H}^k is defined by (72) and the involved constants are defined by (73).

Proof. Since 1) has been shown in Lemma 3, we only prove 2). By $\eta = \beta/\gamma > 1$ in (73) and $\gamma \in (1, \zeta^{-1/k_0})$ in (10),

$$\frac{1}{\gamma^k} = \frac{\gamma}{\gamma-1} \left(\frac{1}{\gamma^k} - \frac{1}{\gamma^{k+1}} \right), \quad \frac{1}{\eta^k} = \frac{\eta}{\eta-1} \left(\frac{1}{\eta^k} - \frac{1}{\eta^{k+1}} \right). \quad (76)$$

For any $k \geq 0$,

$$\sum_{i=1}^m 2\sigma^k t_i \mathbb{E} \|\mathbf{w}_i^{k+1} - \bar{\mathbf{v}}_i^{k+1}\|^2 \stackrel{\text{(32)}}{\leq} 8m\sigma^k \mathbb{E} \|\mathbf{W}^{k+1} - \mathbf{\Pi}^{k+1}\|_F^2 \stackrel{\text{(55)}}{\leq} \frac{8m\sigma^0 C_2 \gamma^k}{\beta} = \frac{8m\sigma^0 C_2}{\beta} \frac{1}{\eta^k}. \quad (77)$$

From Lemma 3, we have $\mathbf{w}_i^k \in \mathbb{N}(2\delta)$ and $\bar{\mathbf{v}}_i^k \in \mathbb{N}(2\delta)$, which yields

$$\|\nabla f_i(\mathbf{w}_i^k)\|^2 \leq n \|\nabla f_i(\mathbf{w}_i^k)\|_\infty^2 \stackrel{\text{(12)}}{\leq} n\varepsilon_i^2(2\delta), \quad \|\mathbf{h}_i^k\|^2 = \frac{\|\mathbf{g}_i^k\|^2}{(\sigma^k t_i)^2} \stackrel{\text{(57)}}{\leq} \frac{n\varepsilon_i^2(2\delta)}{(\sigma^k t_i)^2}. \quad (78)$$

Recall the descent sequence,

$$H(\mathbf{W}^k, \mathbf{V}^k, \boldsymbol{\sigma}^k) := \mathbb{E} \sum_{i=1}^m \left(f_i(\mathbf{w}_i^k) + \frac{\sigma^k t_i}{2} \|\mathbf{w}_i^k - \bar{\mathbf{v}}_i^k\|^2 \right). \quad (79)$$

We decompose its change between two consecutive communication rounds as

$$H(\mathbf{W}^{k+1}, \mathbf{V}^{k+1}, \boldsymbol{\sigma}^{k+1}) - H(\mathbf{W}^k, \mathbf{V}^k, \boldsymbol{\sigma}^k) = \Delta H_\sigma^k + \Delta H_V^k + \Delta H_W^k, \quad (80)$$

where

$$\begin{aligned}
 \Delta H_\sigma^k &:= H(\mathbf{W}^{k+1}, \mathbf{V}^{k+1}, \boldsymbol{\sigma}^{k+1}) - H(\mathbf{W}^{k+1}, \mathbf{V}^{k+1}, \boldsymbol{\sigma}^k), \\
 \Delta H_V^k &:= H(\mathbf{W}^{k+1}, \mathbf{V}^{k+1}, \boldsymbol{\sigma}^k) - H(\mathbf{W}^{k+1}, \mathbf{V}^k, \boldsymbol{\sigma}^k), \\
 \Delta H_W^k &:= H(\mathbf{W}^{k+1}, \mathbf{V}^k, \boldsymbol{\sigma}^k) - H(\mathbf{W}^k, \mathbf{V}^k, \boldsymbol{\sigma}^k).
 \end{aligned} \quad (81)$$

- For ΔH_σ^k , it follows

$$\begin{aligned}
 \Delta H_\sigma^k &\stackrel{\text{(81)}}{=} \mathbb{E} \sum_{i=1}^m \frac{(\sigma^{k+1} - \sigma^k) t_i}{2} \|\mathbf{w}_i^{k+1} - \bar{\mathbf{v}}_i^{k+1}\|^2 \\
 &\stackrel{\text{(15)}}{=} \mathbb{E} \sum_{i=1}^m \frac{(\gamma-1)\sigma^k t_i}{2} \|\mathbf{w}_i^{k+1} - \bar{\mathbf{v}}_i^{k+1}\|^2.
 \end{aligned} \quad (82)$$

• For ΔH_V^k , we have

$$\begin{aligned}
 \Delta H_V^k &\stackrel{(81)}{=} \mathbb{E} \sum_{i=1}^m \frac{\sigma^k t_i}{2} \left(\|\mathbf{w}_i^{k+1} - \bar{\mathbf{v}}_i^{k+1}\|^2 - \|\mathbf{w}_i^{k+1} - \bar{\mathbf{v}}_i^k\|^2 \right) \\
 &= \mathbb{E} \sum_{i=1}^m \frac{\sigma^k t_i}{2} \left(2 \langle \mathbf{w}_i^{k+1} - \bar{\mathbf{v}}_i^{k+1}, \bar{\mathbf{v}}_i^k - \bar{\mathbf{v}}_i^{k+1} \rangle - \|\Delta \bar{\mathbf{v}}_i^{k+1}\|^2 \right) \\
 &\stackrel{(29)}{\leq} \mathbb{E} \sum_{i=1}^m \left(\frac{2\sigma^k t_i}{3} \|\mathbf{w}_i^{k+1} - \bar{\mathbf{v}}_i^{k+1}\|^2 - \frac{\sigma^k t_i}{8} \|\Delta \bar{\mathbf{v}}_i^{k+1}\|^2 \right).
 \end{aligned} \tag{83}$$

• For ΔH_W^k , it follows from $t_i \geq 1$ that

$$\begin{aligned}
 f_i(\mathbf{w}_i^{k+1}) - f_i(\mathbf{w}_i^k) &\stackrel{(17)}{\leq} \langle \nabla f_i(\mathbf{w}_i^k), \Delta \mathbf{w}_i^{k+1} \rangle + \frac{\sigma^k}{8} \|\Delta \mathbf{w}_i^{k+1}\|^2 \\
 &\stackrel{(29)}{\leq} \frac{2}{\sigma^k t_i} \|\nabla f_i(\mathbf{w}_i^k)\|^2 + \frac{\sigma^k t_i}{4} \|\Delta \mathbf{w}_i^{k+1}\|^2.
 \end{aligned} \tag{84}$$

Moreover,

$$\begin{aligned}
 \|\mathbf{w}_i^{k+1} - \bar{\mathbf{v}}_i^k\|^2 - \|\mathbf{w}_i^k - \bar{\mathbf{v}}_i^k\|^2 &= 2 \langle \mathbf{w}_i^{k+1} - \bar{\mathbf{v}}_i^k, \Delta \mathbf{w}_i^{k+1} \rangle - \|\Delta \mathbf{w}_i^{k+1}\|^2 \\
 &\stackrel{(21)}{=} 2 \langle -\mathbf{h}_i^k, \Delta \mathbf{w}_i^{k+1} \rangle - \|\Delta \mathbf{w}_i^{k+1}\|^2 \\
 &\stackrel{(29)}{\leq} 4 \|\mathbf{h}_i^k\|^2 - \frac{3}{4} \|\Delta \mathbf{w}_i^{k+1}\|^2.
 \end{aligned} \tag{85}$$

Combining (84) and (85), we obtain

$$\begin{aligned}
 \Delta H_W^k &\stackrel{(81)}{=} \mathbb{E} \sum_{i=1}^m \left(f_i(\mathbf{w}_i^{k+1}) - f_i(\mathbf{w}_i^k) + \frac{\sigma^k t_i}{2} \left(\|\mathbf{w}_i^{k+1} - \bar{\mathbf{v}}_i^k\|^2 - \|\mathbf{w}_i^k - \bar{\mathbf{v}}_i^k\|^2 \right) \right) \\
 &\stackrel{(84,85)}{\leq} \mathbb{E} \sum_{i=1}^m \left(\frac{2}{\sigma^k t_i} \|\nabla f_i(\mathbf{w}_i^k)\|^2 - \frac{\sigma^k t_i}{8} \|\Delta \mathbf{w}_i^{k+1}\|^2 + 2\sigma^k t_i \|\mathbf{h}_i^k\|^2 \right) \\
 &\stackrel{(78)}{\leq} \mathbb{E} \sum_{i=1}^m \left(\frac{4n\varepsilon_i^2(2\delta)}{\sigma^k t_i} - \frac{\sigma^k t_i}{8} \|\Delta \mathbf{w}_i^{k+1}\|^2 \right) \\
 &\stackrel{(14)}{\leq} \frac{4mn\varepsilon^2(2\delta)}{\sigma^k t_{\min}} - \mathbb{E} \sum_{i=1}^m \frac{\sigma^k t_i}{8} \|\Delta \mathbf{w}_i^{k+1}\|^2.
 \end{aligned} \tag{86}$$

Overall, using (82), (83), and (86), we derive that

$$\begin{aligned}
 H(\mathbf{W}^{k+1}, \mathbf{V}^{k+1}, \boldsymbol{\sigma}^{k+1}) - H(\mathbf{W}^k, \mathbf{V}^k, \boldsymbol{\sigma}^k) &\stackrel{(80)}{=} \Delta H_\sigma^k + \Delta H_V^k + \Delta H_W^k \\
 &\leq -\mathbb{E} \sum_{i=1}^m \left(\frac{\sigma^k t_i}{8} \|\Delta \mathbf{w}_i^{k+1}\|^2 + \frac{\sigma^k t_i}{8} \|\Delta \bar{\mathbf{v}}_i^{k+1}\|^2 \right) + \frac{4mn\varepsilon^2(2\delta)}{\sigma^k t_{\min}} + \mathbb{E} \sum_{i=1}^m \frac{(1+\gamma)\sigma^k t_i}{2} \|\mathbf{w}_i^{k+1} - \bar{\mathbf{v}}_i^{k+1}\|^2 \\
 &\stackrel{(77)}{\leq} -\mathbb{E} \sum_{i=1}^m \left(\frac{\sigma^k t_i}{8} \|\Delta \mathbf{w}_i^{k+1}\|^2 + \frac{\sigma^k t_i}{8} \|\Delta \bar{\mathbf{v}}_i^{k+1}\|^2 \right) + \frac{4mn\varepsilon^2(2\delta)}{\sigma t_{\min}} \frac{1}{\gamma^k} + \frac{4(1+\gamma)m\sigma^0 C_2}{\beta} \frac{1}{\eta^k} \\
 &\stackrel{(76)}{=} -\mathbb{E} \sum_{i=1}^m \left(\frac{\sigma^k t_i}{8} \|\Delta \mathbf{w}_i^{k+1}\|^2 + \frac{\sigma^k t_i}{8} \|\Delta \bar{\mathbf{v}}_i^{k+1}\|^2 \right) + C \left(\frac{1}{\gamma^k} - \frac{1}{\gamma^{k+1}} \right) + D \left(\frac{1}{\eta^k} - \frac{1}{\eta^{k+1}} \right),
 \end{aligned} \tag{87}$$

where C and D are defined by (73). \square

Definition 1 ($L^2(\Omega)$ space). Let $(\Omega, \mathcal{F}, \mathbb{P})$ be a probability space. Define

$$L^2(\Omega) := \{X : \Omega \rightarrow \mathbb{R}^n \text{ measurable} \mid \mathbb{E}\|X\|^2 < \infty\}.$$

Two random variables X and Y are identified if $\mathbb{P}(X = Y) = 1$. For simplicity, write $L^2 := L^2(\Omega)$.

Definition 2 (L^2 -convergence). Let $(\Omega, \mathcal{F}, \mathbb{P})$ be a probability space. Let $\{X_k\}_{k \geq 1}$ and $X \in \mathbb{R}^n$ be random vectors such that

$$\mathbb{E}\|X_k\|^2 < \infty \quad \text{and} \quad \mathbb{E}\|X\|^2 < \infty.$$

We say that X_k converges to X in L^2 (or in mean square) if

$$\lim_{k \rightarrow \infty} \mathbb{E} \|X_k - X\|^2 = 0.$$

Lemma 8. Let $\{\mathbf{w}^k\} \subseteq \mathbb{N}(2\delta)$ be a of random vectors. Suppose there exist constants $c > 0$ and $\gamma > 1$ such that

$$\mathbb{E} \|\mathbf{w}^{k+1} - \mathbf{w}^k\|^2 \leq \frac{c^2}{\gamma^k}, \quad \forall k \geq 0,$$

and let $f : \mathbb{R}^d \rightarrow \mathbb{R}$ be continuously differentiable. Then the following statements are valid.

1) Sequence $\{\mathbf{w}^k\}$ converges (to \mathbf{w}^∞) in L^2 space and sequence $\{\mathbb{E}\mathbf{w}^k\}$ converges, i.e.,

$$\lim_{k \rightarrow \infty} \mathbb{E} \|\mathbf{w}^k - \mathbf{w}^\infty\|^2 = 0, \quad \lim_{k \rightarrow \infty} \mathbb{E}\mathbf{w}^k = \mathbb{E}\mathbf{w}^\infty. \quad (88)$$

2) The nonlinear expectation converges to the function evaluated at the limit:

$$\lim_{k \rightarrow \infty} \mathbb{E} |f(\mathbf{w}^k) - f(\mathbf{w}^\infty)| = 0.$$

3) The sequence satisfies

$$\mathbb{E} \|\mathbf{w}^k - \mathbf{w}^\infty\|^2 = O(\gamma^{-k}), \quad \mathbb{E} |f(\mathbf{w}^k) - f(\mathbf{w}^\infty)| = O(\gamma^{-k/2}).$$

Proof. 1) By the triangle inequality and Cauchy-Schwarz:

$$\|\mathbb{E}\mathbf{w}^{k+1} - \mathbb{E}\mathbf{w}^k\| \leq \mathbb{E} \|\mathbf{w}^{k+1} - \mathbf{w}^k\| \leq \sqrt{\mathbb{E} \|\mathbf{w}^{k+1} - \mathbf{w}^k\|^2} \leq \frac{c}{\gamma^{k/2}}.$$

Since $\sum_{k=0}^{\infty} \gamma^{-k/2} < \infty$, the sequence of means $\{\mathbb{E}\mathbf{w}^k\}$ has summable increments and is thus Cauchy, thus it converges. From the assumption, by Minkowski's inequality in L^2 , for $k > \ell$,

$$\sqrt{\mathbb{E} \|\mathbf{w}^k - \mathbf{w}^\ell\|^2} \leq \sum_{j=\ell}^{k-1} \sqrt{\mathbb{E} \|\mathbf{w}^{j+1} - \mathbf{w}^j\|^2} \leq \sum_{j=\ell}^{k-1} \frac{c}{\gamma^{j/2}} \leq \frac{\sqrt{\gamma}}{\sqrt{\gamma} - 1} \frac{1}{\gamma^{\ell/2}} \rightarrow 0 \quad \text{as } \ell \rightarrow \infty.$$

Therefore, sequence $\{\mathbf{w}^k\}$ is Cauchy in the L^2 space. By the completeness of L^2 , there is \mathbf{w}^∞ satisfying the first condition in (88), which immediately yields

$$\lim_{k \rightarrow \infty} \|\mathbb{E}\mathbf{w}^k - \mathbb{E}\mathbf{w}^\infty\| \leq \lim_{k \rightarrow \infty} \mathbb{E} \|\mathbf{w}^k - \mathbf{w}^\infty\| \leq \lim_{k \rightarrow \infty} \sqrt{\mathbb{E} \|\mathbf{w}^k - \mathbf{w}^\infty\|^2} = 0. \quad (89)$$

2) It is noted that $\{\mathbf{w}^k\}$ is bounded in $\mathbb{N}(2\delta)$ and f is continuously differentiable, so f is Lipschitz continuous on a bounded region containing $\mathbb{N}(2\delta)$ and \mathbf{w}^∞ . This implies that there is a constant $c > 0$ such that

$$|f(\mathbf{w}^k) - f(\mathbf{w}^\infty)| \leq c \|\mathbf{w}^k - \mathbf{w}^\infty\|.$$

Taking the expectation leads to

$$\lim_{k \rightarrow \infty} \mathbb{E} |f(\mathbf{w}^k) - f(\mathbf{w}^\infty)| \leq \lim_{k \rightarrow \infty} c \mathbb{E} \|\mathbf{w}^k - \mathbf{w}^\infty\| \stackrel{(89)}{=} 0. \quad (90)$$

3) Let $N > k$ and consider the difference,

$$\Delta_N := |\mathbb{E} \|\mathbf{w}^N - \mathbf{w}^k\|^2 - \mathbb{E} \|\mathbf{w}^\infty - \mathbf{w}^k\|^2|.$$

We first show $\lim_{N \rightarrow \infty} \Delta_N = 0$. By linearity of expectation and the triangle inequality,

$$\begin{aligned} \Delta_N &\leq \mathbb{E} \left| \|\mathbf{w}^N - \mathbf{w}^k\|^2 - \|\mathbf{w}^\infty - \mathbf{w}^k\|^2 \right| \\ &\leq \mathbb{E} \left(\left| \|\mathbf{w}^N - \mathbf{w}^k\| - \|\mathbf{w}^\infty - \mathbf{w}^k\| \right| (\|\mathbf{w}^N - \mathbf{w}^k\| + \|\mathbf{w}^\infty - \mathbf{w}^k\|) \right) \\ &\leq \mathbb{E} \left(\|\mathbf{w}^N - \mathbf{w}^\infty\| (\|\mathbf{w}^N - \mathbf{w}^k\| + \|\mathbf{w}^\infty - \mathbf{w}^k\|) \right). \end{aligned}$$

Taking expectations of the both sides of the above inequality leads to

$$\begin{aligned} \Delta_N &\leq \mathbb{E} \left(\|\mathbf{w}^N - \mathbf{w}^\infty\| \cdot (\|\mathbf{w}^N - \mathbf{w}^k\| + \|\mathbf{w}^\infty - \mathbf{w}^k\|) \right) \\ &\leq \sqrt{\mathbb{E} \|\mathbf{w}^N - \mathbf{w}^\infty\|^2} \cdot \sqrt{\mathbb{E} (\|\mathbf{w}^N - \mathbf{w}^k\| + \|\mathbf{w}^\infty - \mathbf{w}^k\|)^2} \\ &\leq \sqrt{\mathbb{E} \|\mathbf{w}^N - \mathbf{w}^\infty\|^2} \cdot \left(\sqrt{\mathbb{E} \|\mathbf{w}^N - \mathbf{w}^k\|^2} + \sqrt{\mathbb{E} \|\mathbf{w}^\infty - \mathbf{w}^k\|^2} \right) \\ &\leq d \sqrt{\mathbb{E} \|\mathbf{w}^N - \mathbf{w}^\infty\|^2}, \end{aligned} \quad (91)$$

where the second and third inequalities are from Cauchy-Schwarz inequality and Minkowski's inequality in L^2 , the last inequality holds because the second factor can be bounded by a constant d independent of N due to $\{\mathbf{w}^k\} \subseteq \mathbb{N}(2\delta)$. Then

$$\lim_{N \rightarrow \infty} \Delta_N \stackrel{(91)}{\leq} \lim_{N \rightarrow \infty} d \sqrt{\mathbb{E} \|\mathbf{w}^N - \mathbf{w}^\infty\|^2} \stackrel{(88)}{=} 0,$$

that is

$$\lim_{N \rightarrow \infty} \mathbb{E} \|\mathbf{w}^N - \mathbf{w}^k\|^2 = \mathbb{E} \|\mathbf{w}^\infty - \mathbf{w}^k\|^2. \quad (92)$$

From the telescoping representation

$$\mathbf{w}^N - \mathbf{w}^k = \sum_{j=k}^{N-1} (\mathbf{w}^{j+1} - \mathbf{w}^j),$$

apply Minkowski inequality in L^2 ,

$$\begin{aligned} \sqrt{\mathbb{E} \|\mathbf{w}^\infty - \mathbf{w}^k\|^2} &\stackrel{(92)}{=} \sqrt{\lim_{N \rightarrow \infty} \mathbb{E} \|\mathbf{w}^k - \mathbf{w}^N\|^2} \\ &= \lim_{N \rightarrow \infty} \sqrt{\mathbb{E} \|\mathbf{w}^k - \mathbf{w}^N\|^2} \\ &\leq \lim_{N \rightarrow \infty} \sum_{j=k}^{N-1} \sqrt{\mathbb{E} \|\mathbf{w}^{j+1} - \mathbf{w}^j\|^2} \\ &\leq \lim_{N \rightarrow \infty} \sum_{j=k}^{N-1} \frac{c}{\gamma^{j/2}} = \frac{\sqrt{\gamma}}{\sqrt{\gamma} - 1} \frac{1}{\gamma^{k/2}}. \end{aligned}$$

This immediately shows that

$$\mathbb{E} \|\mathbf{w}^k - \mathbf{w}^\infty\|^2 = O(\gamma^{-k}).$$

Using the above condition and (90), we derive that

$$\mathbb{E} |f(\mathbf{w}^k) - f(\mathbf{w}^\infty)| \leq c \sqrt{\mathbb{E} \|\mathbf{w}^k - \mathbf{w}^\infty\|^2} = O(\gamma^{-k/2}).$$

The proof is finished. \square

E. Proof of Theorem 3

Theorem 3. Let $\{(\mathbf{W}^k, \mathbf{V}^k)\}$ be the sequence generated by Algorithm 1 with Setup 1. Then the following statements hold under Assumptions 1 and 2.

1) For any $i \in [m]$,

$$\lim_{k \rightarrow \infty} \mathbb{E} \|\Delta \mathbf{w}_i^k\| = \lim_{k \rightarrow \infty} \mathbb{E} \|\Delta \bar{\mathbf{v}}_i^k\| = \lim_{k \rightarrow \infty} \mathbb{E} \|\mathbf{w}_i^k - \bar{\mathbf{v}}_i^k\| = 0. \quad (93)$$

2) Sequence $\{\boldsymbol{\varpi}^k\}$ converges to $\boldsymbol{\varpi}^\infty$ in the sense of L^2 convergence and expectation, namely,

$$\lim_{k \rightarrow \infty} \mathbb{E} \|\boldsymbol{\varpi}^k - \boldsymbol{\varpi}^\infty\|^2 = 0, \quad \lim_{k \rightarrow \infty} \mathbb{E} \boldsymbol{\varpi}^k = \mathbb{E} \boldsymbol{\varpi}^\infty. \quad (94)$$

Moreover, sequence $\{(\mathbb{E} \mathbf{W}^k, \mathbb{E} \mathbf{V}^k)\}$ converges and satisfies

$$\lim_{k \rightarrow \infty} \mathbb{E} \mathbf{W}^k = \lim_{k \rightarrow \infty} \mathbb{E} \mathbf{V}^k = (\mathbb{E} \boldsymbol{\varpi}^\infty, \dots, \mathbb{E} \boldsymbol{\varpi}^\infty) =: \mathbf{W}^\infty.$$

3) Three sequences $\{H^k\}$, $\{\tilde{H}^k\}$, and $\{\mathbb{E} f(\boldsymbol{\varpi}^k)\}$ converge to the same value, namely,

$$\lim_{k \rightarrow \infty} \tilde{H}^k = \lim_{k \rightarrow \infty} H^k = \lim_{k \rightarrow \infty} \mathbb{E} f(\boldsymbol{\varpi}^k) = \mathbb{E} f(\boldsymbol{\varpi}^\infty).$$

Proof. 1) From (75) and (74), sequence $\{\tilde{H}^k\}$ is non-increasing and bounded from below. Therefore, it converges. Taking the limit of the both sides of (75) yield

$$\lim_{k \rightarrow \infty} \mathbb{E} \sum_{i=1}^m \left(\frac{\sigma^k t_i}{8} \|\Delta \mathbf{w}_i^{k+1}\|^2 + \frac{\sigma^k t_i}{8} \|\Delta \bar{\mathbf{v}}_i^{k+1}\|^2 \right) = 0,$$

namely, for each $i \in [m]$,

$$\lim_{k \rightarrow \infty} \sigma^k \mathbb{E} \|\Delta \mathbf{w}_i^{k+1}\|^2 = 0, \quad \lim_{k \rightarrow \infty} \sigma^k \mathbb{E} \|\Delta \bar{\mathbf{v}}_i^{k+1}\|^2 = 0, \quad (95)$$

This immediately leads to the first two equations in (93). The third equation in (93) holds due to

$$\sum_{i=1}^m 2t_i \mathbb{E} \|\mathbf{w}_i^k - \bar{\mathbf{v}}_i^k\|^2 \stackrel{(32)}{\leq} 8m \mathbb{E} \|\mathbf{W}^k - \mathbf{\Pi}^k\|_F^2 \stackrel{(55)}{\leq} \frac{8mC_2}{\beta^k}. \quad (96)$$

2) By (95), we conclude that

$$\mathbb{E} \|\Delta \mathbf{w}_i^{k+1}\|^2 = o(\sigma^k) = o(\gamma^{-k}), \quad \forall i \in [m],$$

which indicates that there exists a constant $c_i > 0$ such that

$$\mathbb{E} \|\Delta \mathbf{w}_i^{k+1}\|^2 \leq \frac{c_i^2}{\gamma^k}, \quad \forall i \in [m]. \quad (97)$$

Recall (25) that $\boldsymbol{\varpi}^k = \frac{1}{m} \sum_{i=1}^m \mathbf{w}_i^k$ and Lemma 3 that $\mathbf{w}_i^k \in \mathbb{N}(2\delta)$ for all $i \in [m]$ and $k \geq 0$. It is easy to check $\boldsymbol{\varpi}^k \in \mathbb{N}(2\delta)$ for all $k \geq 0$. Moreover,

$$\|\Delta \boldsymbol{\varpi}^{k+1}\|^2 = \left\| \frac{1}{m} \sum_{i=1}^m \Delta \mathbf{w}_i^{k+1} \right\|^2 \stackrel{(29)}{\leq} \frac{1}{m} \sum_{i=1}^m \|\Delta \mathbf{w}_i^{k+1}\|^2 \stackrel{(97)}{\leq} \frac{\sum_{i=1}^m c_i^2}{m} \frac{1}{\gamma^k}. \quad (98)$$

Therefore, by Lemma 8 1), $\{\boldsymbol{\varpi}^k\}$ converges to $\boldsymbol{\varpi}^\infty$ in the sense of L^2 convergence and $\{\mathbb{E}\boldsymbol{\varpi}^k\}$ converges, and they satisfy (94). By Lemma 8 1) and condition (97), sequence $\{\mathbb{E}\mathbf{w}_i^k\}$ converges. It follows from (96) that

$$\lim_{k \rightarrow \infty} \mathbb{E} \|\mathbf{w}_i^k - \bar{\mathbf{v}}_i^k\|^2 = 0,$$

which by Jensen's inequality results in

$$\lim_{k \rightarrow \infty} \|\mathbb{E}\mathbf{w}_i^k - \mathbb{E}\bar{\mathbf{v}}_i^k\| \leq \lim_{k \rightarrow \infty} \mathbb{E} \|\mathbf{w}_i^k - \bar{\mathbf{v}}_i^k\| \leq \lim_{k \rightarrow \infty} \sqrt{\mathbb{E} \|\mathbf{w}_i^k - \bar{\mathbf{v}}_i^k\|^2} = 0.$$

Therefore, $\lim_{k \rightarrow \infty} \mathbb{E}\bar{\mathbf{v}}_i^k = \lim_{k \rightarrow \infty} \mathbb{E}\mathbf{w}_i^k$ for any $i \in [m]$, thereby

$$\lim_{k \rightarrow \infty} \mathbb{E}\mathbf{W}^k = \lim_{k \rightarrow \infty} \mathbb{E}\mathbf{V}^k.$$

Again by Jensen's inequality,

$$\begin{aligned} \lim_{k \rightarrow \infty} \|\mathbb{E}\mathbf{w}_i^k - \mathbb{E}\boldsymbol{\varpi}^k\| &\leq \lim_{k \rightarrow \infty} \sqrt{\mathbb{E} \|\mathbf{w}_i^k - \boldsymbol{\varpi}^k\|^2} \\ &\stackrel{(26)}{\leq} \lim_{k \rightarrow \infty} \sqrt{\mathbb{E} \|\mathbf{W}^k - \mathbf{\Pi}^k\|_F^2} \stackrel{(55)}{=} 0. \end{aligned}$$

The above two facts suffice to

$$\lim_{k \rightarrow \infty} \mathbb{E}\mathbf{w}_i^k = \lim_{k \rightarrow \infty} \mathbb{E}\boldsymbol{\varpi}^k = \mathbb{E}\boldsymbol{\varpi}^\infty, \quad \forall i \in [m]. \quad (99)$$

3) The convergence of sequence $\{\tilde{H}^k\}$ and (72) can lead to the convergence of sequence $\{H^k\}$ and

$$\begin{aligned} \lim_{k \rightarrow \infty} \tilde{H}^k &= \lim_{k \rightarrow \infty} H^k \stackrel{(72)}{=} \lim_{k \rightarrow \infty} \mathbb{E} \sum_{i=1}^m \left(f_i(\mathbf{w}_i^k) + \frac{\sigma^k t_i}{2} \|\mathbf{w}_i^k - \bar{\mathbf{v}}_i^k\|^2 \right) \\ &\stackrel{(77)}{=} \lim_{k \rightarrow \infty} \mathbb{E} \sum_{i=1}^m f_i(\mathbf{w}_i^k). \end{aligned} \quad (100)$$

From 2), we have shown that $\{\boldsymbol{\varpi}^k\}$ converges (to $\boldsymbol{\varpi}^\infty$) in the sense of L^2 convergence, namely,

$$\lim_{k \rightarrow \infty} \mathbb{E} \|\boldsymbol{\varpi}^k - \boldsymbol{\varpi}^\infty\|^2 = 0,$$

which by Lemma 8 2) contributes to

$$\lim_{k \rightarrow \infty} \mathbb{E}f(\boldsymbol{\varpi}^k) = \mathbb{E}f(\boldsymbol{\varpi}^\infty),$$

and

$$\begin{aligned} \lim_{k \rightarrow \infty} \mathbb{E} \|\mathbf{w}_i^k - \boldsymbol{\varpi}^\infty\|^2 &\leq \lim_{k \rightarrow \infty} 2\mathbb{E} \|\mathbf{w}_i^k - \boldsymbol{\varpi}^k\|^2 + \lim_{k \rightarrow \infty} 2\mathbb{E} \|\boldsymbol{\varpi}^k - \boldsymbol{\varpi}^\infty\|^2 \\ &= \lim_{k \rightarrow \infty} 2\mathbb{E} \|\mathbf{w}_i^k - \boldsymbol{\varpi}^k\|^2 \\ &\stackrel{(26)}{\leq} \lim_{k \rightarrow \infty} 2\mathbb{E} \|\mathbf{W}^k - \mathbf{\Pi}^k\|_F^2 \stackrel{(55)}{=} 0. \end{aligned} \quad (101)$$

This means sequence $\{\mathbf{w}_i^k\}$ converges to $\boldsymbol{\varpi}^\infty$ in the sense of L^2 convergence. Therefore, by Lemma 8 2), we obtain

$$\lim_{k \rightarrow \infty} \mathbb{E}f_i(\mathbf{w}_i^k) = \mathbb{E}f_i(\boldsymbol{\varpi}^\infty), \quad \forall i \in [m].$$

This together with (100) gives rise to

$$\lim_{k \rightarrow \infty} \tilde{H}^k = \lim_{k \rightarrow \infty} H^k = \lim_{k \rightarrow \infty} \mathbb{E} \sum_{i=1}^m f_i(\mathbf{w}_i^k) = \mathbb{E} \sum_{i=1}^m f_i(\boldsymbol{\varpi}^\infty) = \mathbb{E} f(\boldsymbol{\varpi}^\infty).$$

This finishes the proof. \square

F. Proof of Theorem 4

Theorem 4. *Let $\{(\mathbf{W}^k, \mathbf{V}^k)\}$ be the sequence generated by Algorithm 1 with Setup 1. Then under Assumptions 1 and 2,*

$$\mathbb{E} \|\mathbf{W}^k - \mathbf{W}^\infty\|_F^2 = O(\gamma^{-k}), \quad \mathbb{E} \|\mathbf{V}^k - \mathbf{W}^\infty\|_F^2 = O(\gamma^{-k}), \quad \mathbb{E} |f(\boldsymbol{\varpi}^k) - f(\boldsymbol{\varpi}^\infty)| = O(\gamma^{-k/2}).$$

Proof. The first result follows from (97), (101), and Lemma 8 3). The second result follows from

$$\begin{aligned} \mathbb{E} \|\mathbf{V}^k - \mathbf{W}^\infty\|_F^2 &\leq 2\mathbb{E} \|\mathbf{W}^k - \mathbf{W}^\infty\|_F^2 + 2\mathbb{E} \|\mathbf{V}^k - \mathbf{W}^k\|_F^2 \\ &\stackrel{(32)}{\leq} 2\mathbb{E} \|\mathbf{W}^k - \mathbf{W}^\infty\|_F^2 + \frac{8m}{t_{\min}} \mathbb{E} \|\mathbf{W}^k - \boldsymbol{\Pi}^k\|_F^2 \\ &\stackrel{(55)}{\leq} 2\mathbb{E} \|\mathbf{W}^k - \mathbf{W}^\infty\|_F^2 + \frac{8mC_2}{t_{\min}} \frac{1}{\beta^k} \\ &\leq 2\mathbb{E} \|\mathbf{W}^k - \mathbf{W}^\infty\|_F^2 + \frac{8mC_2}{t_{\min}} \frac{1}{\gamma^k} \\ &= O(\gamma^{-k}). \end{aligned}$$

The last result holds because of (98) and Lemma 8 3). \square